

UC Riverside

UC Riverside Electronic Theses and Dissertations

Title

Initial Design of a Dual Fluidized Bed Reactor

Permalink

<https://escholarship.org/uc/item/3cj2w18x>

Author

Yun, Minyoung

Publication Date

2014

Peer reviewed|Thesis/dissertation

UNIVERSITY OF CALIFORNIA
RIVERSIDE

Initial Design of a Dual Fluidized Bed Reactor

A Thesis submitted in partial satisfaction
of the requirements for the degree of

Master of Science

in

Chemical and Environmental Engineering

by

Minyoung Yun

March 2014

Thesis Committee:

Dr. Joseph Norbeck, Chairperson

Dr. Akua Asa-Awuku

Dr. David Cocker

Copyright by
Minyoung Yun
2014

The Thesis of Minyoung Yun is approved:

Committee Chairperson

University of California, Riverside

Acknowledgement

Firstly, I would like to thank my research advisor, Dr Joseph Norbeck for his guidance. I consider myself very lucky that I had his guidance throughout the course of this study. I would not have come all the way to here without his help. I would also like to thank Dr Chan Seung Park for his support and suggestions. Dr Dal Hee Bae who was a visiting scholar in 2012 provided excellent technical knowledge in terms of the reactor design. The project for the design of DFB was successfully completed with Dr Park and Dr Bae's guidance. I also deeply appreciate the guidance of Dr Wayne Miller about technical parts of the reactor. I would also like to thank my committee members, Dr David Cocker and Dr Akua Asa-awuku for their support.

I would like to thank my amazing colleagues for their guidance and suggestions. I would like to thank Dr Xiaoming Lu for his guidance regarding simulation work of Steam hydro-gasification. Mr. Noam Hart encouraged me to get through this graduate course. I would also like to thank Mr. Junior Castillo for their help throughout the construction of the cold model DFB.

Last, but not the least, I would like to thank my family to be supportive through past 2.5 years. I would also like to thank my boyfriend for his supports and encouragements. I also appreciate the supports from friends in my year, Noam Hart, Diep Vu, Talin Avanesian, John Matsubu, Alicia Talyor and Matt Kale.

ABSTRACT OF THE THESIS

Initial Design of a Dual Fluidized Bed Reactor

by

Minyoung Yun

Master of Science, Graduate Program in Chemical and Environmental Engineering

University of California, Riverside, March 2014

Dr. Joseph Norbeck, Chairperson

Steam hydro-gasification (SH) of biomass holds great potential to produce transportable and storable fuels to replace fossil fuel. There is a critical task which needs to be addressed in order to scale up the process. SH is an endothermic reaction which requires external heat to operate. The use of two highly coupled reactors: one for SH and the other for combustion of solid feedstock may provide sufficient and efficient heat management and produce an outlet product with high carbon conversion. A dual fluidized bed (DFB) gasifier has been selected for this purpose. A cold mode DFB was built with acrylic plastic to simulate the gasifier in order to develop insight for the optimization of the reactor for SH. This is the main objective of my thesis. Hydrodynamics tests were carried out to better understand the solid flow behavior in the cold mode DFB. The mixing test found that the gases from two reactors within the cold DFB mixed in the fast bed. The mixing level decreased with increase in the gas velocity in the fast bed and the BFB. Also the degree of gas mixing decreased with the increase in solid inventory. The hydrodynamics test found that increase in the gas velocity in the fast bed and the BFB leads to increase in the solid holdup

in the fast bed. This same trend was observed with the three sizes of sand. Design modifications are made to improve the design of DFB for SH based on the cold model studies. Heat and mass balance of SH in the DFB was calculated using the Aspen plus simulation tool. Combustion of 13.8% of char from SH produces the required heat for SH with the net heat duty of -0.4kw, when 1 dry ton/ day of pine wood is fed into SHR. The results of these studies are presented in the thesis and will contribute to the development of the dual fluidized bed reactor optimized for SH with a potential for commercialization of the process.

Table of contents

Chapter 1 Introduction.....	1
1.1 Fossil fuel and the need for renewable energy.....	1
1.2 Steam hydro-gasification and the CE-CERT process.....	3
1.3 Fluidized bed.....	9
1.4 Objective of this thesis.....	12
1.5 Thesis outline.....	13
Reference.....	14
Chapter 2 Design and construction of cold mode DFB and characterization.....	17
2.1 Design of a cold mode Dual Fluidized Bed reactor (DFB).....	18
2.2 Mixing test.....	25
2.3 Hydrodynamics of cold mode DFB.....	32
2.4 Summary.....	42
2.5 Potential implication of this cold model study.....	43
Reference.....	44
Chapter 3 Modification of DFB design for Stem Hydro-gasification.....	46

3.1 Design optimization for SH.....	46
Reference.....	51
Chapter 4 Simulation of SH in the DFB and future study.....	53
4.1 A heat and mass balance of SH in the DFB.....	53
4.2. Future study.....	56
Reference.....	58
Chapter 5 Summary.....	59

List of Figures

Figure 1.1 U.S. primary energy consumption by fuel, 1980-2040 (U.S. Energy Information Administration Annual Energy Outlook 2014 Early Release Overview).....	2
Figure 1.2 Schematic of CE-CERT process based on SHR (Zhongzhe Liu, 2013).....	4
Figure 1.3 Schematic of CE-CERT process based on SE-SHR (Zhongzhe liu, 2013).....	6
Figure 1.4 The concept of a circulation of heat and mass between a gasifier and a combustor.....	8
Figure 1.5 Schematic of a bubbling bed gasifier (Prabir Basu, 2006).....	10
Figure 1.6 Schematic of a circulating fluidized bed gasifier (Prabir Basu, 2006).....	11
Figure 2.1 The schematic of a dual fluidized bed gasifier.....	18
Figure 2.2 Schematic of the cold mode DFB.....	19
Figure 2.3 Photograph of the cold mode DFB set up.....	20
Figure 2.4 Principle of the DFB process developed by Vienna University of Technology (Christoph Pfeifer, 2008).....	24
Figure 2.5 Conception of the devised pyrolytic gasification plant developed by Ishikawajima-Harima Heavy Industries Co., Japan (Takahiro Murakami, 2007).....	24
Figure 2.6 Effect of inlet gas velocities of (a) the fast bed and (b) the bubbling fluidized bed on gas mixing behaviors: Ar concentration in the gas stream exiting from the fast bed.....	31

Figure 2.7 Effect of solid inventory in the loop seal (BFB) on gas mixing behaviors: Ar concentration in the gas stream exiting from the fast bed.....	32
Figure 2.8 Different gas- solid flow regimes. (A) A bubbling fluidized bed, (B) turbulent fluidization, (C) a circulating fluidized bed, (D) Pneumatic transport condition.....	36
Figure 2.9 Hydrodynamics of bed particles at flow rate of 350 ft ³ /hr at (a) the mixer and (b) the upper bed.....	38
Figure 2.10 Hydrodynamics of bed particles at flow rate of 400 ft ³ /hr at (a) the mixer and (b) the upper bed.....	39
Figure 2.11 Hydrodynamics of bed particles at flow rate of 450 ft ³ /hr at (a) the mixer and (b) the upper bed.....	40
Figure 2.12 Hydrodynamics of bed particles of 150µm at flow rate of 350~450 ft ³ /hr at (a) the mixer and (b) the upper bed.....	41
Figure 3.1 Original DFB design and new design with modifications.....	46
Figure 4.1 Schematic flow diagram of 1TPD SHR with combustor.....	54

List of Tables

Table 2.1 Dimension of the cold mode DFB.....	21
Table 2.2 Properties of bed material and fluidizing gases.....	26
Table 2.3 Case 1 Cold mode, U_{mf} and U_t of bed materials in hydrogen and oxygen condition at 25°C, 14.7psi.....	29
Table 2.4 Case scenario 2) hot mode, U_{mf} and U_t based on the flue gas and CO ₂	29
Table 2.5 Conditions for hot flue gas.....	30
Table 2.6 Test variables for the hydrodynamics test.....	33
Table 2.7 Particle size distribution of 150, 200, 250 µm sand group.....	34
Table 2.8 Minimum fluidizing velocities and terminal velocities for silica sand with various sizes.....	35
Table 4.1 Proximate and ultimate analysis of pinewood.....	53
Table 4.2 Steam tables of simulation results.....	55
Table 4.3 Char formation ratio and heat balance at temperature of 700~850 oC (Xiaoming Lu, 2012).....	56

Chapter 1 Introduction

1.1 Fossil fuel and the need for renewable energy

Fossil fuel energy is a non-renewable resource because it requires millions of years for fossil fuel to accumulate. Fossil fuels include coal, oil, and natural gas. The demand for fossil fuel derived energy has stayed at a high level for previous decades. The time for fossil fuels to accumulate cannot keep up with the rapid extraction rate. The depletion of fossil fuels has become a future challenge (Mikael Hook, 2013). The dependence on fossil fuel in 2012 stayed high despite the constant efforts to move away from fossil fuel by the countries in the Organization for Economic Co-operation and Development (OECD) (<http://www.worldwatch.org/fossil-fuels-dominate-primary-energy-consumption-1>). Majority (87 percent) of the total energy consumption in 2012 is reported to come from fossil fuel. Coal consumption in China increased by 6.1%. India showed a 9.9% increase in 2012. This considerable growth of coal consumption in the two large countries significantly attributed to the increase in fossil fuel energy consumption in the year. The Energy Information Administration (EIA) forecasts fossil fuels will still be used to meet over three quarters of the total energy demand in the United States in 2040 as Fig 1.1 illustrates. The share of total U.S energy for renewable energy is expected to increase by only 2%.

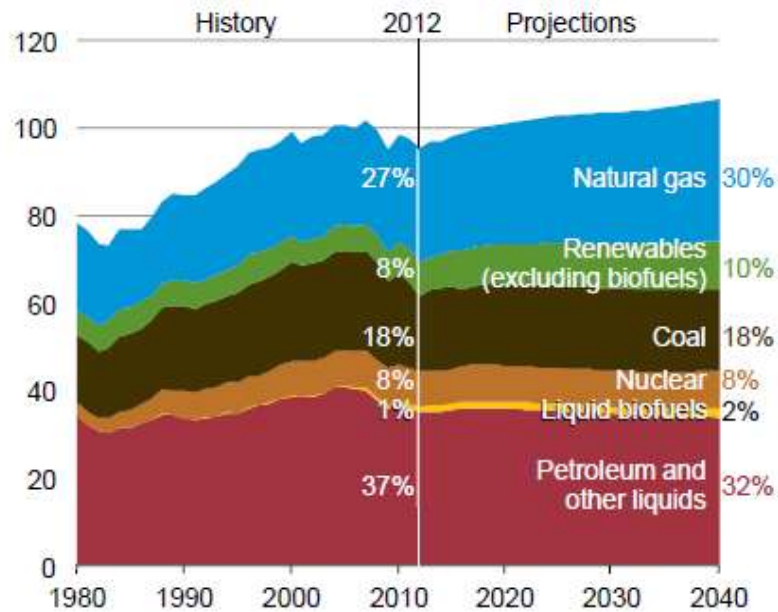


Figure 1.1 U.S. primary energy consumption by fuel, 1980-2040 (U.S. Energy Information Administration | Annual Energy Outlook 2014 Early Release Overview)

The world reliance on fossil fuel causes a problem which is green house gas (CO₂) emission. Nearly three fourth of CO₂ emissions caused by human activity are known to come from the consumption of fossil fuel energy (<http://energy.gov/science-innovation/energy-sources/fossil>).

Growing concerns about the depletion of fossil fuel and CO₂ emission have driven worldwide attention to renewable energy source such as biomass (Christopher Koroneos, 2013). Biomass is plant based material derived from living or recently deceased organisms (http://www.biomassenergycentre.org.uk/portal/page?_pageid=76,15049&_dad=portal). Biomass use contributes little or no net carbon dioxide to the atmosphere (P.M Lva, 2004). It is an attractive way to produce storable and transportable fuels from biomass. The use of biomass as an energy source is possible only with a technology to produce energy from

biomass at a competitive price. The introduction of the technology will reduce the dependency on fossil fuels.

1.2 Steam hydro-gasification and the CE-CERT process

Hydro gasification is a reaction of feedstocks with hydrogen to produce gaseous hydrocarbons with high energy value. This technology had gained attention since the 1930s. It has an advantage that the process does not require an expensive oxygen plant. However this technology did not see much industrial success because of its slow reaction rate which requires the use of a catalyst.

Steam hydro gasification (SH) developed by the Center for Environmental Research & Technology (CE-CERT), University of California Riverside (UCR) overcomes the slow reaction rate by introducing steam as a gasifying agent. The steam works as a co-gasifying agent with hydrogen (Zhongzhe Liu, 2013, N Gardner, 1974). This advanced technology achieves higher rate of methane formation with the introduction of steam. It can also use feedstock with high moisture and low energy content such as biomass (Jeon SK, 2007). SH holds possibility for biomass utilization to produce renewable energy for this reason.

SH is a thermo chemical process accompanied with steam and H₂ as a gasifying agent. The reaction occurs at moderate temperatures (750°C~850°C) in a pressurized reactor, producing methane rich fuel gas. SH is an important part of the CE-CERT process which is presented in Fig 1.2.

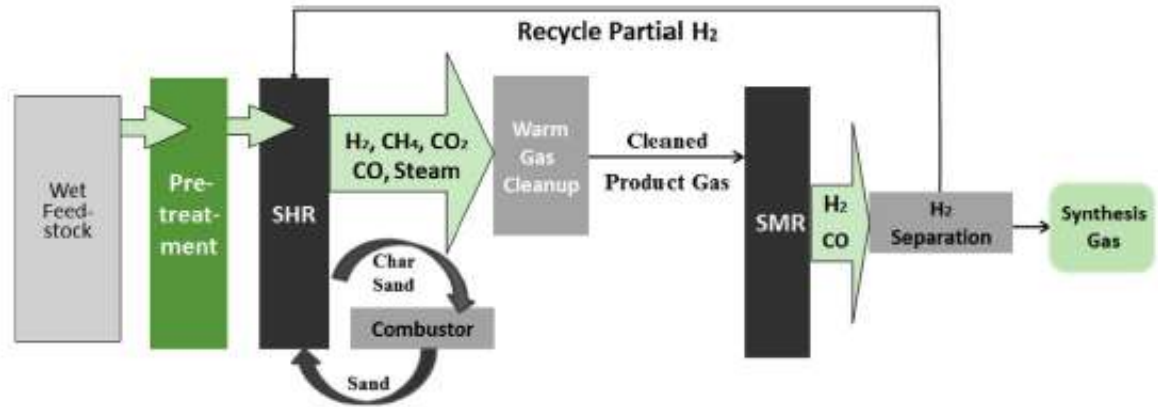
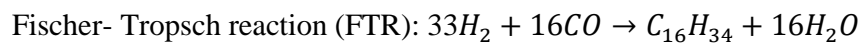
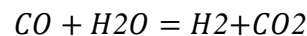
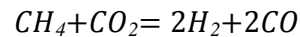
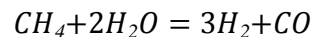
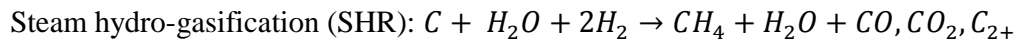


Figure 1.2 Schematic of CE-CERT process based on SHR (Zhongzhe Liu, 2013)

The CE-CERT process consists of four main reactors coupled to each other consecutively: a feedstock pretreatment unit (FPU), a steam hydro-gasification reactor (SHR), a steam methane reforming reactor (SMR) and a Fischer-Tropsch reactor (FTR). Initially the feedstock is processed to become a pumpable slurry in the FPU. The slurry is fed into the SHR with hydrogen and steam by a progressive cavity pump. It is converted into methane rich fuel gas consisting mainly of CH_4 , H_2 , CO , and CO_2 in the SHR (Xiaoming Lu, 2012). The product gas from the SHR goes through the gas cleanup process at 350°C for the removal of impurities such as sulfur and nitrogen compounds (H_2S , COS , etc) (Kim K, 2007, 2010). The cleaned product gas is transported to the SMR to produce synthesis gas for the FTR. The SHR coupled with the SMR does not require an external hydrogen supply because sufficient hydrogen is generated to be sent back to the SHR (Zhongzhe Liu, 2013). The synthesis gas is transferred to the last step, the FTR. Finally, the FTR generates the desired product, Fischer-Tropsch diesel fuel and waxes. It should be noted that this whole process is carried out without external H_2

supply with a closed-loop H₂ cycle. This is one of main advantageous features of the process.

The reactions taking place in three reactors (SHR, SMR, and Fischer-Tropsch reactor) are explained as followed (Raju ASK, 2008):



Previous research by the SH group found that SH showed greatly improved gasification efficiency in terms of the rate of reaction. Carbon conversion is also higher compared to dry hydro gasification. The kinetics of product gas formation of SH was estimated to be as high as 30 times greater at 1043K (S.K. Jeon, 2007). Furthermore, the unique feature of utilization of wet feedstock brings several advantages over a conventional steam gasification process. Firstly, feedstock does not need a drying process. This not only reduces the operational cost but also simplifies the overall process. Second of all, the water content in wet feedstock turns into steam and works as a gasifying agent in a gasifier. This reduces the potential energy loss from generation and transportation of steam from outside the gasifier.

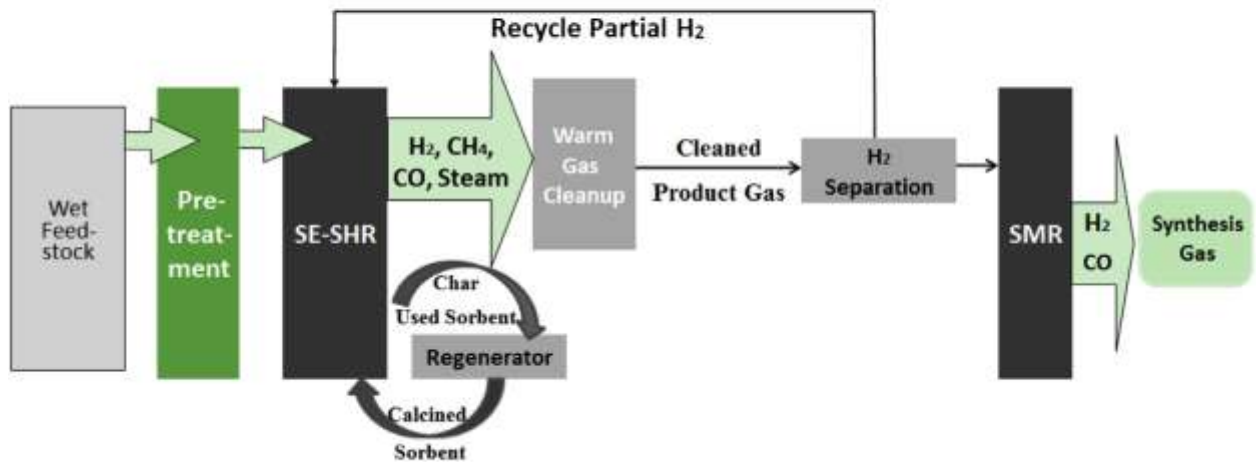


Figure 1.3 Schematic of CE-CERT process based on SE-SHR (Zhongzhe liu, 2013)

The control of green house gas (CO_2) emission is an important factor for an energy generation technology considering potential environmental impacts as mentioned above. Schematic of SE-SHR process in Fig 1.3 illustrates the upgraded CE-CERT process with a regenerator. The generated CO_2 is removed by calcined sorbent within the SHR. The used sorbent is regenerated in the regenerator. This sorption enhanced (SE) technique alters the equilibrium to result in the production of gases with higher energy value. Previous research by SH group found the addition of calcined sorbent not only promotes CO_2 removal in the SHR but also enhances hydrogen and methane production. (Zhongzhe Liu, 2013)

These advantages of steam hydro-gasification and previous experiments by SH group show promise for a commercialization of the technology. There is one more important task to be addressed for the implementation of the process. SH is an endothermic reaction which requires energy to bring the temperature of reactants up to

the reaction temperatures (700~850°C). Also, the heat is used to sustain the process (Norbeck JM, 2012). Electric heaters can supply the required heat for SH in a lab scale gasifier. However the heat must be provided without an external heater in a self sustainable way for a pilot or commercial scale reactor. The necessary heat for the gasification can be generated from combustion of remaining char or part of feedstocks from SH. The generated heat can be supplied to the SH gasifier in two ways, directly or indirectly. The two methods for heat transportation are described in detail below.

a. Direct heat supply

Combustion and gasification occur in one reactor, and the necessary heat is directly supplied for gasification within the reactor. A good example is the partial oxidation reaction (POX). POX has several advantages over other energy production technologies. For example, one of the advantages of POX is high operating temperature and pressure compared to steam reforming. Additionally, this reaction can employ a bifunctional catalyst for combustion and steam reforming (Ann M. De Groote, 1996). Although POX technology has met with some success of an industrial commercialization, it faces some challenges. A POX reactor needs high operational cost for the separation of carbon dioxide from a product gas. A careful process control is also very important because gasification and combustion take place in one reactor (S.K. Jeon, 2007). Moreover, when air is utilized as an oxygen source for combustion, POX has a disadvantage of a dilution of a product gas with nitrogen. This results in a significantly reduced heating value of the product gas.

b. Indirect heat supply

Combustion and gasification take place in two separate reactors respectively unlike the direct heat supply method. The heat of combustion is transported to a gasifier through a circulation of bed material such as sand, olivine, and dolomite etc. A high heating value of a product gas is guaranteed because the produced gas is not diluted with CO_2 or N_2 . This concept of heat transfer can be achieved with a dual bed reactor consisting of two reactors. One is for a gasifier and the other is for a combustor. The concept is presented in Fig 1.4.

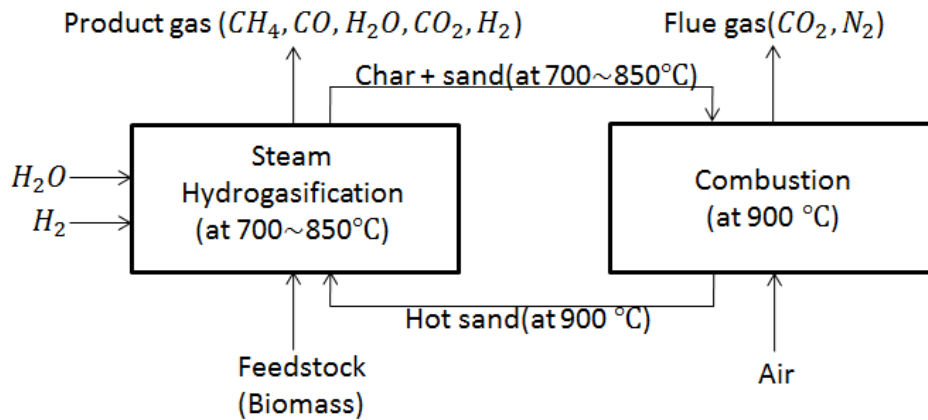


Figure 1.4 The concept of a circulation of heat and mass between a gasifier and a combustor

A dual bed reactor was chosen to achieve the heat supply without the penalty for SH. Here the penalty means the disadvantages that POX has for example the dilution of a product gas with nitrogen or carbon dioxide. A fluidized bed reactor was selected to

achieve the circulation of heat within a dual bed reactor. The features of fluidized beds are elaborated upon in the following section.

1.3 Fluidized bed

A fluidized bed is a type of reactor in which solid particles exhibit a fluid-like behavior. This reactor has been industrially utilized because of its good heat and mass transfer characteristics. Fluidized-bed reactors are found in a wide range of applications in various industrial operations. The operations are chemical, petroleum, mineral, and pharmaceutical industries (Prabir Basu, 2006. Veeraya Jiradilok, 2006, Sebastian Zimmermann, 2005).

Fluidized bed gasifiers offer higher gasification efficiency over fixed bed gasifiers as the feedstocks are mixed thoroughly and vigorously. This enables an excellent gas-particle contact (L.M. Armstrong, 2011). Also, there are several more advantages. Firstly, fluidized bed gasifiers have a uniform temperature profile throughout a bed which makes the control of temperature easy. Second of all, these gasifiers are suitable for many kinds of feedstocks for example low rank coal, agricultural residues, food waste and biomass. Last but not the least, the bed ash in a fluidized gasifier does not form an agglomeration due to its low operation temperature (700~850°C). This makes the ash removal process simple and affordable. Fluidized bed gasifiers are widely utilized in the coal and biomass gasification industries for these advantages.

Fluidized gasifiers are classified into the following two major types, elaborated upon in the following section 1.5, 1.6.

1. Bubbling fluidized bed gasifiers (BFB) (Figure 1.5)
2. Circulating fluidized bed gasifiers (CFB) (Figure 1.6)

1.3.1. Bubbling fluidized bed gasifier

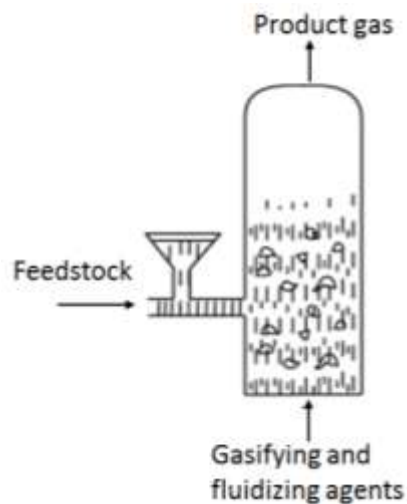


Figure 1.5 Schematic of a bubbling bed gasifier (Prabir Basu, 2006)

A typical BFB gasifier is made up of a furnace. The furnace contains a bubbling bed of granular solids and a freeboard above it. BFB gasifiers are also called stationary or slow fluidized beds. (Prabir Basu, 2006).

Feedstock enters the reactor in either overbed or inbed method into a bubbling fluidized bed gasifier. It is transported into the reactor by either a screw feeder or a lock

hopper. Fluidizing and gasifying agents are fed at the bottom of the furnace. The fluidizing and gasifying agents include air, steam, and carbon dioxide. Solid particles are normally fluidized at the superficial gas velocity of 0.5~2.5m/s in a bubbling fluidized regime. The entrained small particles into a freeboard mostly return to the bed. If not, the particles which leave a bubbling bed gasifier are captured by cyclones or filter bags. Intense solid-solid mixing occurs in the bubbling bed, while intense solid-gas mixing happens in the freeboard. Most of solid-gas reaction occurs in a solid bed and gas-gas reaction happens in a freeboard for this reason. The relatively low gas velocity and big particle size of bed material ensure a long residence time of feedstock in the gasifier. This results in high gasification efficiency.

1.3.2 Circulating fluidized bed gasifier

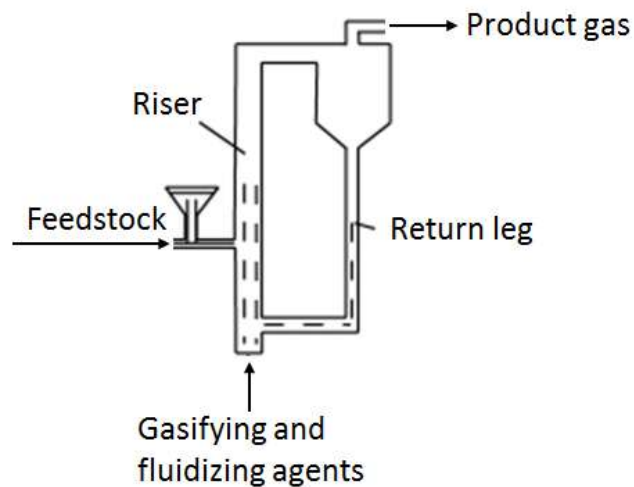


Figure 1.6 Schematic of a circulating fluidized bed gasifier (Prabir Basu, 2006)

A typical circulating fluidized bed comprises a riser, a cyclone, and a return leg. Feedstock is transported into a reactor using a lock hopper or a screw feeder by either an inbed or overbed method. Gasifying and fluidizing agents are fed to the bottom of a riser. Large portion of bed particles start entraining a bed at the higher velocity than the terminal velocity of bed particles. Bed particles are usually fluidized at a gas velocity of 4~6 m/s in a riser in a fast regime. The gasification reaction between solids and gases occurs throughout the riser. This is a main difference from a bubbling fluidized bed gasifier. Entrained unreacted carbon and bed material are captured in a cyclone and sent back to a riser through a return leg. This ensures a high carbon conversion.

CFBs have several advantages such as high throughput and high heat and mass transfer besides the high carbon conversion. CFBs are widely utilized for both catalytic and non-catalytic reactors in the chemical process industries for these advantages (Thatchai Samruamphianskun, 2012).

These both of fluidized bed gasifiers (BFB and CFB) have great features for SH. Therefore main features from both of the reactors were employed for the SHR design. CFB enables a circulation of heat and mass between a gasifier and a combustor in the configuration. BFB accommodates a large volume of bed solids which ensure effective heat transfer. As a result, a special type of reactor called a dual fluidized bed (DFB) was selected for the SHR. It has the advantages of both of the fluidized bed gasifiers. The detailed design of cold and hot mode DFB is presented in the following chapter.

1.4 Objective of this thesis

The overall objective is to develop and optimize a model of a dual fluidized bed (DFB) for steam hydro-gasification. This research will contribute to a scale up of CE-CERT steam hydro-gasification process in a dual fluidized bed. First of all, a full understanding of bed hydrodynamics in a DFB must be gained to achieve the goal. A cold mode DFB was designed and constructed for this purpose. Furthermore hydrodynamics studies were designed and carried out in the cold model DFBs. The results of these studies can be utilized for the design of a hot mode DFB. Secondly, the original DFB design was modified to improve the gasifier for steam hydro-gasification. The modification was suggested based on the experience gained throughout the cold model studies. Lastly, a heat and mass balance of SH in a DFB was calculated. These objectives are elaborated upon below:

1. The first objective aims to study the bed hydrodynamics in a DFB reactor. A cold mode DFB was designed for SH and constructed for this study. The goal is to optimize the hydrodynamics conditions to achieve high gasification efficiency. This provides foundational data for an interpretation of steam hydro-gasification performance in a DFB setting. The experiments for the characterization of hydrodynamics in a DFB were designed and carried out. The tests are to identify the effects of major parameters on bed hydrodynamics such as particle size of bed material, solid inventory, and superficial gas velocity. The performance was defined and evaluated with a level of interchange of gases between two reactors within a DFB setting. Solid hold up was also measured in different parts of the cold mode DFB. The bed hydrodynamics behavior in the cold mode setting is studied to assist in the optimization of a DFB design for SH.

2. The second objective of this thesis is to improve the original design of DFB for SH. Important observations were gained during the cold model studies. Parts of the cold DFB had a need to be improved. These parts are modified to improve the DFB for SH in terms of solid circulation.

3. The last objective is to calculate a heat and mass balance of SH in the DFB using the aspen simulation. This is to confirm the operability of SH in the DFB on a commercial scale.

1.5 Thesis outline

Chapter 2 provides a design of a cold mode DFB reactor. It also presents the experimental results from the hydrodynamics study. Chapter 3 gives an improved design of the DFB for SH. Chapter 4 presents simulation result of SH in the DFB. It also presents a future study related to this research. Lastly, Chapter 5 provides the overall summary and conclusions.

References

Ann M. De Groote, Gilbert F. Froment, Simulation of the catalytic partial oxidation of methane to synthesis gas, *Applied Catalysis A: General* 138, 1996, 245-264

Raju ASK. Production of synthetic fuels using syngas from a steam hydro gasification and reforming process. University of California Riverside; 2008

Kim K, Park N. Removal of hydrogen sulfide from a steam-hydrogasifier product gas by zinc oxide sorbent: effect of non-steam gas components. *J Ind Eng Chem* 2010;16:967-72

Kim K, Park N. Effect of non-steam component of steamhydrogasifier product gas upon sulfidation of zinc oxide sorbent. *Korean J Chem Eng* 2010;27:1715-7

Kim K, Jeon SK, Vo C, Park CS, Norbeck JM. Removal of hydrogen sulfide from a steam-hydrogasifier product gas by zinc oxide sorbent. *Ind Eng Chem Res* 2007;46:5848-54

N Gardner, E Samuels, K Wilks, *Catalyzed Hydrogasification of Coal Chars*, Adv. Chem. Ser, 1974, ACS Publications

Zhongzhe Liu, Chan S. Park, Joseph M. Norbeck, Sorption enhanced steam hydrogasification of coal for synthesis gas production with in-situ CO₂ removal and self-sustained hydrogen supply, *International journal of hydrogen energy* ,38, 2013, 7016-7025

P.M Lva, Z.H Xionga, J Changa, C.Z Wua, Y Chena, J.X Zhub. An experimental study on biomass Air-steam gasification in a fluidized bed. *Bioresource Technology*. 2004:95-101

Xiaoming Lu, Joseph M. Norbeck, Chan S. Park. Production of Fischer Tropsch fuels and electricity from bituminous coal based on steam hydrogasification. *Energy*. 2012:525-531

S.K. Jeon, C.S. Park, C.E. Hackett, J.M. Norbeck. Characteristics of steam hydrogasification of wood using a micro-batch reactor. Fuel. December 2007:2817-23

L.M. Armstrong, S. Gu , K.H. Luo., Effects of limestone calcination on the gasification processes in a BFB coal gasifier, chemical engineering journal, April 2011: 848-860

Norbeck JM, Park CS, Raju AS. US patent application 2012022235

Prabir Basu. Combustion and Gasification in Fluidized Beds. 2006: 211p

Thatchai Samruamphianskun, Pornpote Piumsomboon, Benjapon Chalermssinuwon. Computation of system turbulences and dispersion coefficients in circulating fluidized bed, Chemical Engineering Research and Design, Volume 90, Issue 12, December 2012, Pages 2164–2178

Veeraya Jiradiloka, Dimitri Gidaspowb,*, Somsak Damronglerda, William J. Kovesc, Reza Mostofic, Kinetic theory based CFD simulation of turbulent fluidization of FCC particles in a riser, Chemical Engineering Science 61 (2006) 5544 – 5559

Sebastian Zimmermann and Fariborz Taghipour, CFD Modeling of the Hydrodynamics and Reaction Kinetics of FCC Fluidized-Bed Reactors, Ind. Eng. Chem. Res. 2005, 44, 9818-9827

Christopher Koroneos , Thomas Spachos, Nikolaos Moussiopoulos,, Exergy analysis of renewable energy sources, Renewable Energy. 2003, 28, 295–310

Mikael Hook, XuTang, Depletion of fossil fuels and anthropogenic climate change—A review, Energy Policy, 52(2013)797–809

<http://energy.gov/science-innovation/energy-sources/fossil>

<http://www.worldwatch.org/fossil-fuels-dominate-primary-energy-consumption-1>

U.S. Energy Information Administration | Annual Energy Outlook 2014 Early Release
Overview

http://www.biomassenergycentre.org.uk/portal/page?_pageid=76,15049&_dad=portal

Chapter 2 Design and construction of cold mode DFB and characterization

One of the most important features that effects gasification efficiency in a fluidized bed is flow behavior hydrodynamics. The hydrodynamics mainly influences reactions in a fluidized bed. Hydrodynamics makes it possible to control and optimize the solid mixture and flow pattern in a fluidized bed reactor (Vaccaro, S, 1997). Solid flow between two reactors in a DFB gasifier directly affects gasification efficiency. To understand and control the heat and mass transportation between a gasifer and a combustor is crucial to the operation of gasification and its efficiency (Takahiro Murakami, 2007). Understanding the hydrodynamics of a fluidized bed reactor is essential for finding the correct operating parameters for the appropriate fluidization regime (Sebastian Zimmermann, 2005).

A number of hydrodynamics studies were conducted in a cold model fluidized bed reactor in the past. Hydrodynamics study conducted in cold models provides the basis for a design and especially operation of a fluidized bed system (A. Charitos, 2010). Solid movement behavior in the DFB setting should be closely investigated for a successful design and operation of the DFB for SH. A cold mode DFB was designed and built by our group for these reasons. The experimental studies were designed and conducted with varying parameters such as solid inventory, superficial gas velocity, and particle size.

2.1 Design of a cold mode Dual Fluidized Bed reactor (DFB)

The dual fluidized bed reactor designed by the SH group employs the main feature of both of a CFB and a BFB. The schematic of the DFB is depicted in Fig 2.1. DFB has a feature of a circulating fluidized bed reactor (CFB) as can be seen in the Fig 2.1 (Christoph Pfeifer, 2008). And it also has a bubbling fluidized bed in the configuration.

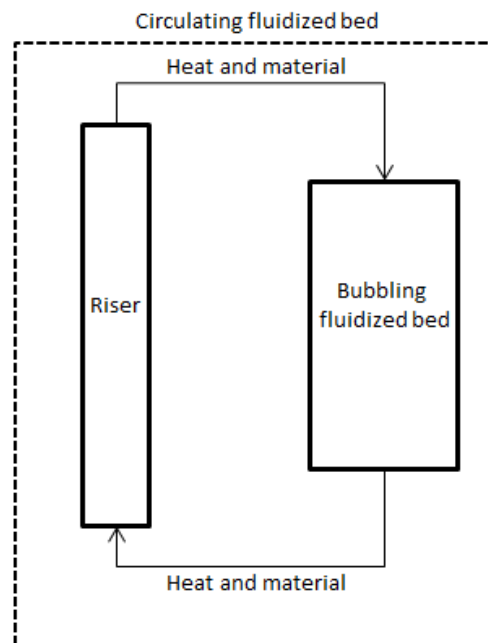
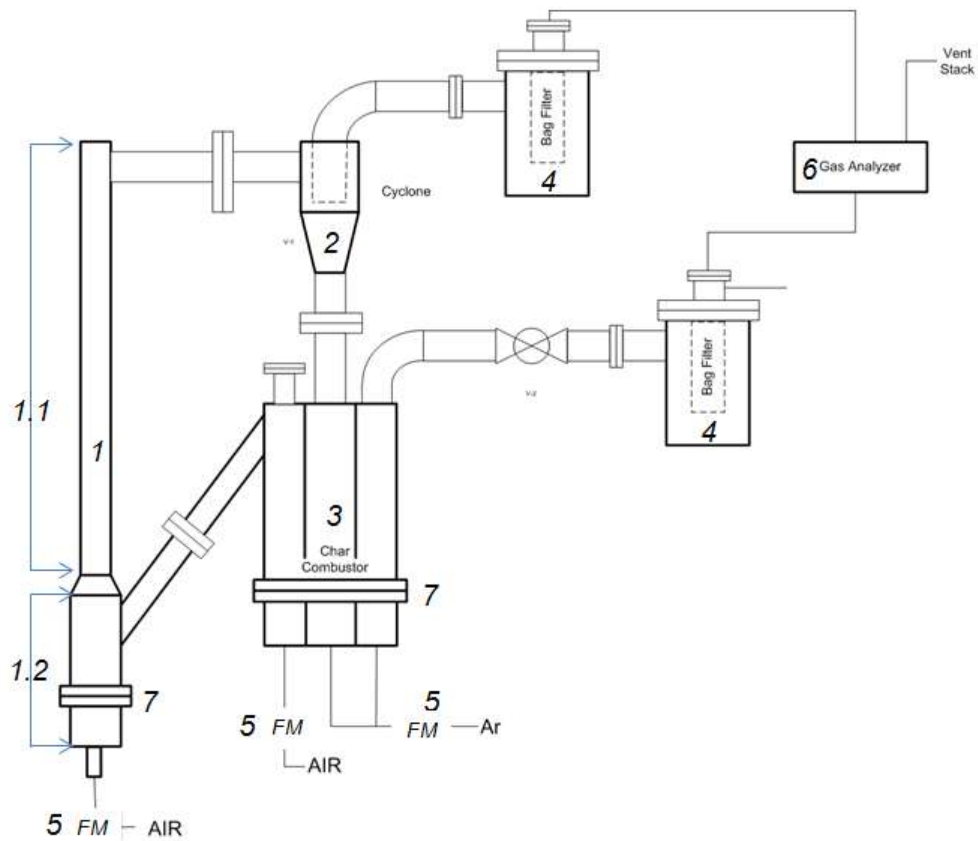


Figure 2.1 The schematic of a dual fluidized bed gasifier

The DFB is made up of a riser and a BFB. Heat and bed material circulate between the two furnaces. The circulation of mass carries necessary heat for SH. The suggested design concept was elaborated and simulated with a cold mode facility built

with acrylic plastic. This cold model DFB was used to study the fundamental hydrodynamics. Here hydrodynamics indicates the solid movement behavior. A schematic diagram of the cold mode DFB is presented in Fig 2.2. A photograph of the cold mode DFB set up is shown in Fig 2.3. The dimensions are given in Table 2.1.



1. Fast bed 1.1 Upper bed 1.2 Mixer 2.Cyclone 3.Bubbling fluidized Bed (BFB)
4.Bag filter 5.Flow Meter (FM) 6.Gas analyser (RGA) 7.Gas distributor

Figure 2.2 Schematic of the cold mode DFB

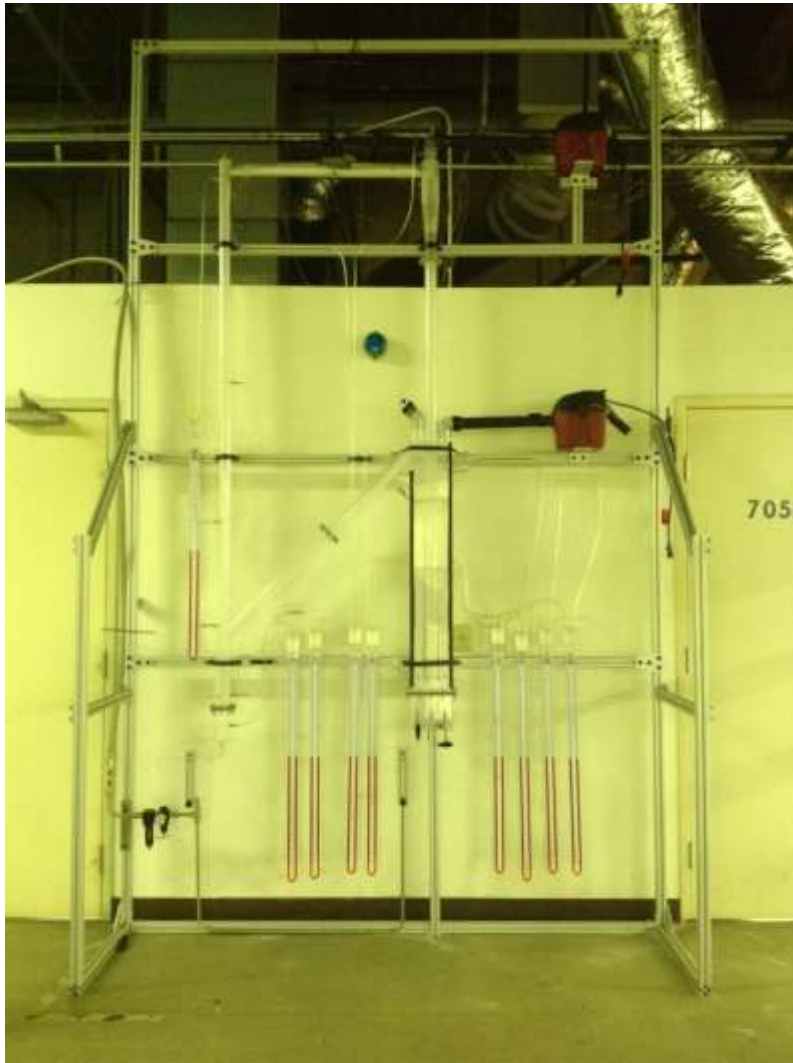


Figure 2.3 Photograph of the cold mode DFB set up

Table 2.1 Dimension of the cold mode DFB

Dimension		Unit
D_{mixer}	0.0508	m
$D_{\text{upper bed}}$	0.042	m
D_{BFB}	0.0508	m
h_{fast}	2	m
h_{BFB}	1	m
d_s	150~242	μm
ρ_s	2650	kgm^{-3}
ρ_G	1.17	kgm^{-3}

The fast bed is divided into two sections: mixer and upper bed as can be seen in Fig. 2.2. The mixer has a wider width compared to the upper bed. The wider volume of the mixer is suitable for solid particles to be vigorously mixed at a low superficial velocity. The upper bed with a narrower width has a good condition for two purposes. The superficial gas velocity in the upper bed is higher than in the mixer because of the narrow width. Gases and solid particles mix together vigorously at the high gas velocity. Secondly, solid particles are easily transported out of the upper bed at the high superficial gas velocity. The fast bed is connected to the BFB with a cyclone which is designed to capture the entrained bed materials and feedstock. This prevents loss of solids. BFB is made of three compartments, each connected to other parts of the reactor. The very left part is connected to the fast bed. The middle part is connected to the cyclone. The very right compartment is connected to the low exit pipe.

Flow meters are installed at the bottom of both of the fast bed and BFB. The volumetric flow rate of the inlet gases is controlled by using the flow meters. Air and argon are chosen as a fluidizing gas for the hydrodynamics study in the cold mode facility. A total nine pressure manometers are installed to measure the pressure drop in different areas in the DFB. The measured pressure differences are used to calculate the solid hold up. Solid holdup here means the amount of solid particles.

The fluidizing gases (Air and argon) are injected at the bottom of the fast bed and the BFB. Air is injected at a high volumetric flow rate to the fast bed. The high volumetric flow rate of air fluidizes the bed of solids in the fast fluidization regime in the fast bed. Air and argon are injected into the BFB. Solid particles in the BFB are fluidized in the bubbling flow regime. These two different gas streams (Air and argon) from the two fluidized beds exhaust the DFB separately. One stream from the fast bed exits through the cyclone. The other stream from the BFB exits through the lower exit line. Two filter bags are installed at the end of two exit lines. The filter bags are installed in order to separate entrained solid particles from the gas streams. The exiting gas streams from both fluidized beds are lastly transported to a gas analyzer (Residual Gas Analyzer (RGA)).

The fast bed is designed for steam hydro-gasification. The BFB is designed for combustion of the remaining char which is generated from gasification. The necessary heat for SH is generated from combustion of chars in the BFB (combustor). The generated heat is transported to the fast bed (gasifier) by a means of circulation of bed material in the hot mode DFB gasifier setting.

A distinctive feature of this reactor is how the loop seal is installed in the configuration. The circulation movement of bed particles is controlled by a loop with a valve in most gas solids process. However, the circulation control by a valve in the SHR is either impossible or highly expensive (T. M. Knowlton , 2012). A special valve that functions under high pressure and temperature condition should be installed. The installation of the valve increases the capital and maintenance cost. This reactor is equipped without a valve. Instead, a loop seal which is a non mechanical solids flow device is installed between the gasifier and the combustor. The use of this type of loop seal eliminates the disadvantages from using a valve. The loop seal is connected to a stand pipe in the configuration. A stand pipe is a pipe through which solids flow by gravity. The stand pipe is located between the cyclone and the BFB. Additionally, this loop seal is incorporated into the BFB that simplifies the overall design by combining two units (a reactor and a loop seal) into one. This eliminates the need for an external loop seal. An example of a gasifier with an external loopseal is given below.

The Fig 2.4 presents the example of a gasifier with an external loop. In this case, a circulation loop of the bed material is created between these two zones to deliver the heat for the gasification process. Heat is transported via the circulating bed material (Christoph Pfeifer, 2008). Additionally and mainly, the loop seal works as a seal between two zones to prevent mixing of gasification gases and combustion gases. This external loop seal is an additional unit to the reactor. This adds complexity to the design and increases costs for maintenance.

Several designs for a DFB with an internal loop seal have been made in previous studies. The internal loop is inserted either in a gasifier or a combustor. A DFB with an internal loop seal does not have the disadvantages accompanied with an external loopseal. One example is given in Fig 2.5. This fluidized bed reactor consists of a BFB gasifier and a pneumatic transported riser (PTR) char combustor. The combustor tube immersed in the bed of solids of the BFB gasifier works as a loop seal as can be seen in Fig 2.5 (Takahiro Murakami, 2007). This design has an advantage from using an internal and integrated form of loop seal. The advantage is the simplification of the overall design of the reactor. However flue gas and product gas can get mixed easily in this condition because a gasifier and a combustor are combined in one reactor. Precious product gas is diluted with combustion flue gas, CO₂ and N₂, in this case.

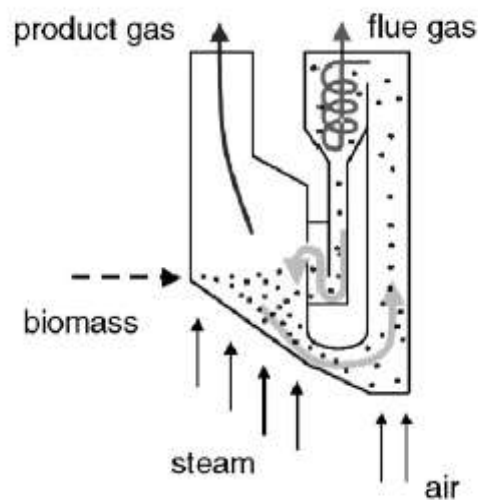


Figure 2.4 Principle of the DFB process developed by Vienna University of Technology (Christoph Pfeifer, 2008)

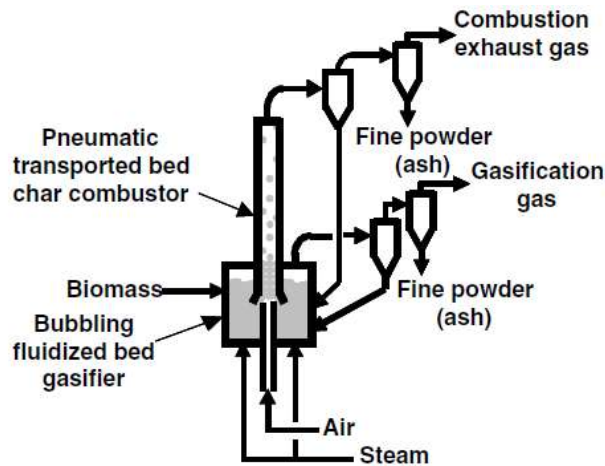


Figure 2.5 Conception of the devised pyrolytic gasification plant developed by Ishikawajima-Harima Heavy Industries Co., Japan (Takahiro Murakami, 2007)

The internal loop seal in the DFB for SH allows for relatively simple operation, low possibility for operational malfunction, and low maintenance cost. A gasifier and a combustor are separated in the setting. This design of a gasifier and a combustor apart enables a low degree of mixing of the combustion flue gas (CO_2 and N_2) and the steam hydro-gasification product gas.

Important experimental studies were carried out using the cold model DFB. A mixing test was designed and carried out to check the degree of mixing of two gases. Also, the test is designed to find the operational variables at which the degree of interchange of two gases is minimized. Additionally, bed hydrodynamics experiments were conducted to study the flow behavior at the different fluidizing parameters. The parameters include superficial gas velocity in the fast bed and the BFB and bed particle size. Air and argon were used for both of experimental studies in a cold model DFB.

These gases were chosen since they do not have overlaps in the peaks of their mass spectra. This provides a convenient way to measure the level of mixing of two gases.

2.2 Mixing test

Gas mixing tests were carried out to examine the level of mixing of the gases from the two reactors (fast bed and BFB) under different fluidization conditions. Compressed air was injected to the fast bed and left compartment of the BFB as the fluidizing gas. Industrial grade argon gas was injected to the right and middle compartments of the BFB. A pure stream of Air from the fast bed and Argon from the BFB are expected to be detected if there is no gas mixing in the configuration. Therefore, the percentage of Ar in the gas flow exiting the fast bed indicates the degree of mixing of the two gases. A residual gas analyzer (RGA) [Cirrus, MKS] with quadruple mass head was used to analyze the exhaust gas streams from the fast bed and the BFB. Silica (OK-75, US Silica) sand with 150 μm average diameter was used as a bed material. The concentration of Air and Ar were determined based on the mass number of 28 and 40 using mass spectrometer (RGA). Physical characteristics of the bed material and the fluidizing gases are shown in Table 2.2.

Table 2.2 Properties of bed material and fluidizing gases

Bed material (silica sand, OK-75)

Particle diameter (D_p) 150~242.5 μm

Skeletal density (ρ_s) 2650 $\text{kg}\cdot\text{m}^{-3}$

Bulk density (ρ_b) 1250 $\text{kg}\cdot\text{m}^{-3}$

Fluidizing gas (Air and Ar at atmospheric condition)

Density ($\rho_{g, \text{Air}}$) 1.18 $\text{kg}\cdot\text{m}^{-3}$

Viscosity ($\mu_{g, \text{Air}}$) 1.76×10^{-5} $\text{kg}\cdot\text{m}^{-1}\cdot\text{sec}^{-1}$

Density ($\rho_{g, \text{Ar}}$) 0.74 $\text{kg}\cdot\text{m}^{-3}$

Viscosity ($\mu_{g, \text{Ar}}$) 2.23×10^{-5} $\text{kg}\cdot\text{m}^{-1}\cdot\text{sec}^{-1}$

The operating range of the volumetric flow rate of Air and Ar was determined based on minimum fluidization velocity (U_{mf}) and terminal velocity (U_t) of bed material of 150 μm silica sand for this experiment. The equations used for the calculations for U_{mf} , U_t are listed in below;

$$\frac{1.75}{\varepsilon_{mf}^3 \Phi_s} \left(\frac{d_p U_{mf} \rho_g}{\mu} \right)^2 + \frac{150(1-\varepsilon_{mf})}{\varepsilon_{mf}^3 \Phi_s^2} \left(\frac{d_p U_{mf} \rho_g}{\mu} \right) = \frac{d_p^3 \rho_g (\rho_s - \rho_g) g}{\mu^2} \quad (1)$$

$$d_p^* = d_p \left[\frac{\rho_g (\rho_s - \rho_g) g}{\mu^2} \right]^{1/3} \quad (2)$$

$$U_t^* = \left[\frac{18}{(d_p^*)^2} + \frac{2.335 - 1.744 \Phi_s}{(d_p^*)^{0.5}} \right]^{-1} \quad (3)$$

$$U_t = U_t^* \left[\frac{\mu (\rho_s - \rho_g) g}{\rho_g^2} \right]^{1/3} \quad (4)$$

U_{mf} of $150\mu m$ sand in the BFB is calculated by Equation (1), while U_t in the fast bed reactor is obtained from equations (2)-(4) (Daizo Kunii, 1991). Where, d_p means particle diameter of the sand (m), ρ_g is gas density (kg/m^3), ρ_s is particle density (kg/m^3), μ is gas viscosity ($kg/m \cdot s$), ε_{mf} is void fraction at fluidizing conditions, Φ_s is sphericity of a particle, d_p^* is dimensionless particle diameter, U_t^* is dimensionless terminal velocity of a falling particle.

The potential implication here means how this cold model study should be interpreted for the hot mode DFB operation. There are two case scenarios. The first case is that hydrogen and oxygen are used instead of air and argon. The kind of gases changes only from argon and air to hydrogen and oxygen. Other condition such as temperature and pressure are the same. This case study was carried out to see how the experiments with air and argon are relevant to the real experiment condition with hydrogen and oxygen. The second case study is to investigate the relationship in the hot mode SH condition. Hot mode SH condition means that

the operation temperature is 700°C. The pressure is 150 psi. U_{mf} and U_t of bed material under the two conditions are calculated in order to establish the relationship between cold studies to both of the cases. Density and viscosity of a mixture of hot gases are also calculated for the U_{mf} and U_t calculation. The calculations are presented below;

$$\rho_m = \frac{(\rho_1 * V_1 + \rho_2 * V_2 + \dots + \rho_n * V_n)}{(V_1 + V_2 + \dots + V_N)}$$

Where,

ρ_m = density of the gas mixture (kg/m³, lb/ft³)

$\rho_1 \dots \rho_n$ = density of each of the components (kg/m³, lb/ft³)

$V_1 + V_2 + \dots + V_N$ = volume share of each of the components (m³, ft³)

$$Vis_m = \frac{\sum_{i=1}^n y_i \times Vis_i}{\sum_{j=1}^n y_j \times \phi(i,j)}$$

$$\phi(1,2) = \frac{(1 + (\frac{vis_1}{vis_2})^{0.5} \times (\frac{M_2}{M_1})^{0.25})^2}{(8 \times (1 + \frac{M_1}{M_2}))^{0.5}}$$

$\phi(i,j) = 1$ when $i=j$

Where,

y_i = mole fraction

vis_1 = viscosity

M_i = molecular weight

U_{mf} and U_t in the case 1 scenario is given in Table 2.3. Here, air is replaced with hydrogen, and argon is replaced with oxygen. The U_{mf} and U_t of oxygen and argon condition does not differ from each other. For example, U_{mf} of oxygen is 2.13 cms^{-1} and one of argon is 1.93 cms^{-1} . U_{mf} and U_t of hydrogen are about 2.5 to 3 times higher than U_{mf} and U_t of air.

Table 2.3 Case 1 Cold mode, U_{mf} and U_t of bed materials in hydrogen and oxygen condition at 25°C, 14.7psi

	H ₂	Air	O ₂	Ar
$U_{mf}(\text{cms}^{-1})$	4.91	2.35	2.13	1.93
$U_t(\text{cms}^{-1})$	379.93	122.3	114.44	102.8

The calculation for the second case is presented in Table 2.4. Hot product gas conditions are given in Table 2.5. The results regarding hot product gas is gained using the Aspen simulation tool. The product gas is a product of the simulated steam hydro-gasification of lignite coal at 700°C, 150 psi. U_{mf} and U_t under the product gas and CO₂ condition each are about 45% smaller than the ones of Air and Ar.

Table 2.4 Case scenario 2 hot mode, U_{mf} and U_t based on the flue gas and CO_2

	Product gas (700°C,150psi)	Air (25°C,14.7psi)	CO_2 (700°C,150psi)	Ar (25°C, 14.7psi)
U_{mf} (cms ⁻¹)	1.12	2.35	1.07	1.93
U_t (cms ⁻¹)	79.6	122.3	56.6	102.8

Table 2.5 Conditions for hot product gas

	Value	Unit
Particle size	150	μm
Temperature	700	°C
Pressure	10	bar
Product gas composition	H ₂ (27%), CO (18%), CO ₂ (8.8%), H ₂ O (54.9%), CH ₄ (6.8%)	

Results and discussion

Gas mixing test in a DFB

Increasing gas velocity by 66% (when $U_{upper\ bed} / U_t$ increased from 3.2 to 4.7) in the fast bed resulted in a decrease in argon from 9.4 to 4.21% about 44.6%. This can be seen in Figure 2.6 (a). This means lower degree of mixing of gases from 9.4 to 4.21%. Argon decreases from 4.8% to 4.2% by 11.6 % with a 23% increase in gas velocity ($U_{BFB} / U_{mf} =$

5.5~6.8) in the BFB as can be seen in Figure 2.6 (b). It was found during the experiments that as the flow rate of Air in the BFB increases, the vigorous Air flow in the BFB prevents for the argon flow to enter the fast bed. This interruption by air resulted in a lower argon amount in the fast bed. The change in air flow rate in the fast bed and the BFB influences the mixing behavior of two gases between two reactors. Increase in the gas flow rate in both the fast bed and BFB lowers the degree of mixing.

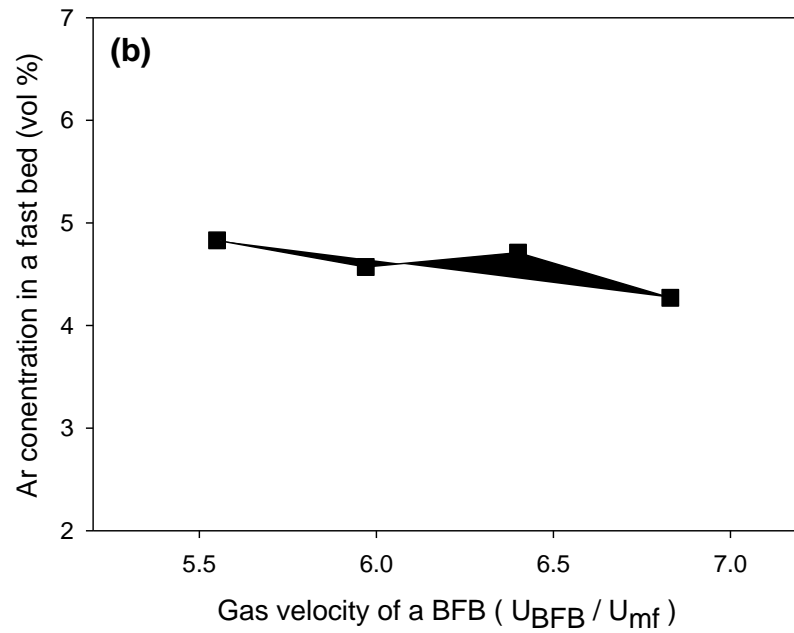
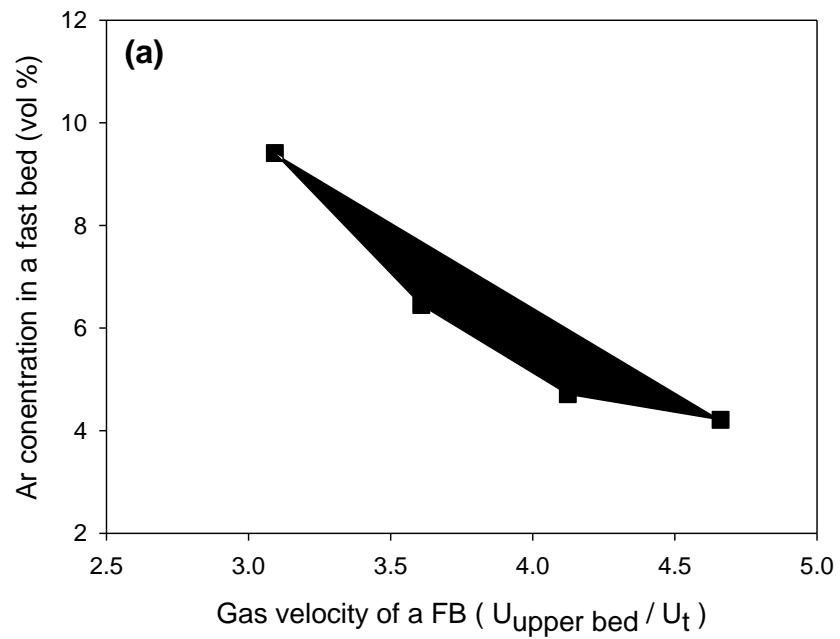


Figure 2.6 Effect of inlet gas velocities of (a) the fast bed and (b) the bubbling fluidized bed on gas mixing behaviors: Ar concentration in the gas stream exiting from the fast bed

The change in the solid inventory in the loop seal decreases the interchange of two gases. The percentage of Ar decreases from 5.49% to 3.85% with increasing solid inventory from 11 to 14kg in Figure 2.7.

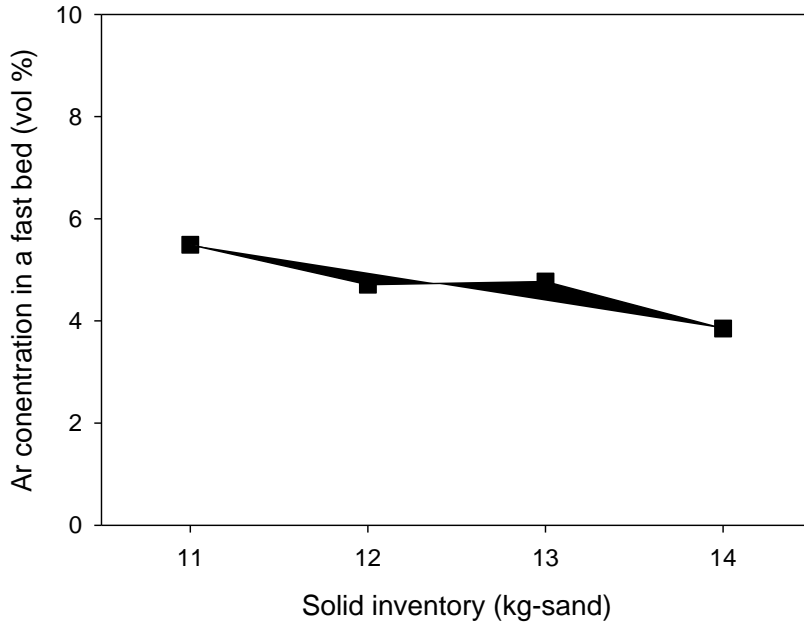


Figure 2.7 Effect of solid inventory in the loop seal (BFB) on gas mixing behaviors: Ar concentration in the gas stream exiting from the fast bed

Gas mixing degree decreased as the gas velocity increased in the fast bed and BFB. Increase in solid inventory also prevents the gas mixing in the configuration. The degree of mixing decreased from maximum 9.4% to minimum 3.8% with increasing gas velocity in the fast bed and the BFB and increasing solid inventory. The range of gas increase in the fast bed is $U_{FB}/U_t = 3.2\sim 4.7$. The range of gas increase in the BFB is $U_{BFB}/U_{mf} = 5.5\sim 6.8$. Solid inventory increased from 11~14kg. To sum up, minimum gas interchange is achieved with highest gas velocity in both fast bed ($U_{FB}/U_t = 4.7$) and BFB ($U_{BFB}/U_{mf} = 6.8$) and highest solid inventory (14kg) within the acceptable range.

2.3 Hydrodynamics of cold mode DFB

Hydrodynamics experimental studies were carried out to investigate the change in the solid hold up under varying fluidizing conditions. The conditions include changes in superficial gas velocity and solid particle sizes. The solid behavior in the fast bed was investigated. It is because the fast bed is designed as a gasifier for SH. The purpose of this test is to study the influence of fluidizing parameters on the solid behavior in the gasifier. A total 36 sets of experiment were conducted. The solid flow behavior in the fast bed was investigated with an increase and decrease in the superficial gas velocity in the fast bed and the BFB. Three different sizes of bed particles were used. The superficial gas velocity here is defined as a gas velocity in both the FB and the BFB.

Pressure manometers were installed at 0.04, 0.32, 2.17 m high from the distributor to measure the solid hold up in the fast bed. A fresh batch of sand was weighed and introduced into the BFB before each test. Test variables are given in Table 2.6.

Table 2.6 Test variables for the hydrodynamics test

Condition	Value	Unit
Flow rate in FB (Air)	350,400,450	SCFH
Flow rate in BFB (Ar+Air)	110,140,170,200	SCFH
Avg size of sand	150,200(214.4),250(242.5)	μm
Inventory	12	Kg

Table 2.7 Particle size distribution of 150, 200, 250 μm sand group

150 Size(μm)	(%)	200 Size(μm)	(%)	250 Size(μm)	(%)
600	0	850	0	860	0
425	0.6	600	0.2	600	0
300	4.2	425	4	425	4.4
212	16.5	300	22	300	40.6
150	45	212	36	212	35
106	29	150	30	150	15.5
75	4.4	106	7	106	4
53	0.3	75	0.5	75	0.3
600	0	53	0.2	53	0.1

Particle size distribution for three sizes of sand is given in Table 2.7. It should be noted that the average size of bed material does not represent every particle sizes in the group. The average size of a group of particle matches with the 50% of bed particle size. The other 50% of particles have about 33% bigger and smaller size as the average size. For example, 150 μm sand group contains 45% of 150 μm particles and the other part of particles are 212, 106 μm . These particles with bigger and smaller diameter also defined the influence of a group of sand on the solid movement behavior.

Calculated minimum fluidizing velocities and terminal velocities of silica sands are presented in Table 2.8.

Table 2.8 Minimum fluidizing velocities and terminal velocities for silica sand with various sizes

Particle size (μm)	150		200 (214.4)		250 (242.5)	
Fluidizing Gas (-)	Air	Ar	Air	Ar	Air	Ar
u_{mf} ($\text{cm}\cdot\text{sec}^{-1}$)	2.38	1.87	4.87	3.83	6.22	4.90
u_t ($\text{cm}\cdot\text{sec}^{-1}$)	55.00	50.30	89.11	86.46	103.49	102.61

Minimum fluidization velocity (U_{mf}) and terminal velocity (U_t) are important parameters in this hydrodynamic test. U_{mf} is an important parameter because a pack of bed particles becomes fluidized at U_{mf} . Bed particles reach equilibrium velocity at the terminal velocity (U_t). These two main velocities is a good indication of the gas-solid flow regime. Different flow regimes divided by U_{mf} and U_t are presented in Fig 2.8. The accurate prediction for a flow regime based on U_{mf} and U_t leads to a successful operation of a fluidized bed reactor. (Abbas H. Sulaymon, 2013).

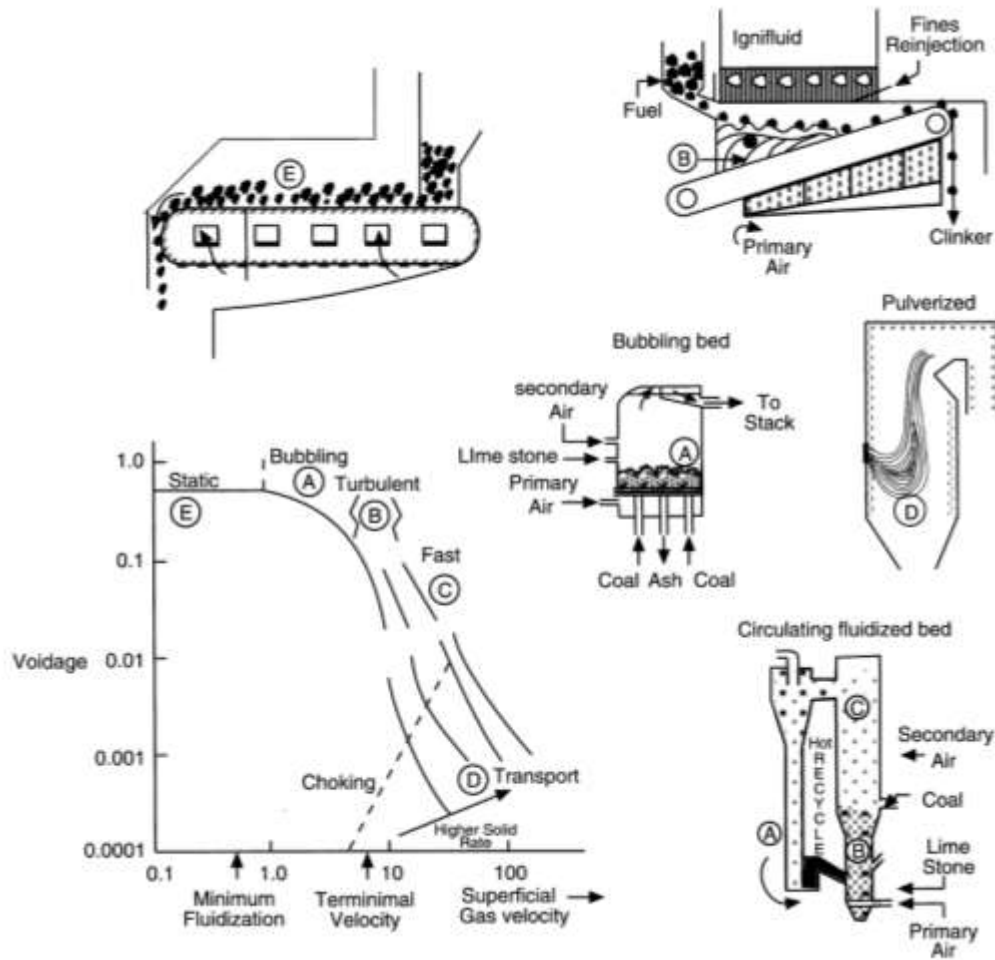


Figure 2.8 Different gas- solid flow regimes

Superficial gas velocity and bed particle size are main fluidizing parameters that influence the solid behavior. Different flow regimes are formed with sands with three different sizes both in the mixer and the fast bed. The expected flow regimes in the mixer and upper bed are presented in Table 2.9.

Table 2.9 Flow regimes with bed materials of 150, 200, 250 μ m in the mixer and the upper bed

			350ft ³ /hr		400ft ³ /hr		450ft ³ /hr	
Size (μ m)	U_t (m/s)	U_{mf} (m/s)	Mixer (1.04m/s)* ^a	Upper bed (1.98m/s)	Mixer (1.19m/s)	Upper bed (2.27m/s)	Mixer (1.34m/s)	Upper bed (2.55 m/s)
250	1.03	0.062	B/T	F	B/T	F	B/T	F
212	0.89	0.048	B/T	F	B/T	F	B/T	F
150	0.55	0.023	T	F	F	F	F	F

* T: Turbulent regime, F: Fast regime, B: Bubbling regime, *a: superficial velocity (m/s)

These results were obtained based on both U_t and U_{mf} of three sizes of sand. The flow regime changes depending on not only the particle size but also the superficial gas velocity as shown in Table 2.9. This is why the particle size and superficial gas velocity were chosen as a test variable to study hydrodynamics in this cold mode DFB.

Results and discussion

Hydrodynamics of bed particles in the cold model DFB, Relationship between solid hold up and superficial gas velocity

Figure 2.9 shows the bed fluid behavior at 350 SCFH air flow rate in the fast bed and 110~200SCFH flow rate in the BFB. Firstly, the increase in the solid hold up was observed in

both the upper bed and the mixer with increasing gas velocity in the BFB for all three sizes of sand. The solid hold up with 150 μm sand increased from 0 to 0.14kg in the mixer, 0~0.12kg in the upper bed. 200 μm sand increased from 0 to 0.34kg in the mixer, 0~0.27kg in the upper bed. The sand group with 250 μm increased from 0 to 0.35kg in the mixer 0 to 0.24kg in the upper bed. Under this gas flow condition, it is speculated that most of the 150 μm sand entrained the fast bed due to low U_t . Most of particles in both 200 and 250 μm group were suspended in either bubbling or turbulent regime in the fast bed due to the high U_t . This explains the reason why less amount of 150 μm sand group resides in the fast bed compared to 200, 250 μm under the same condition.

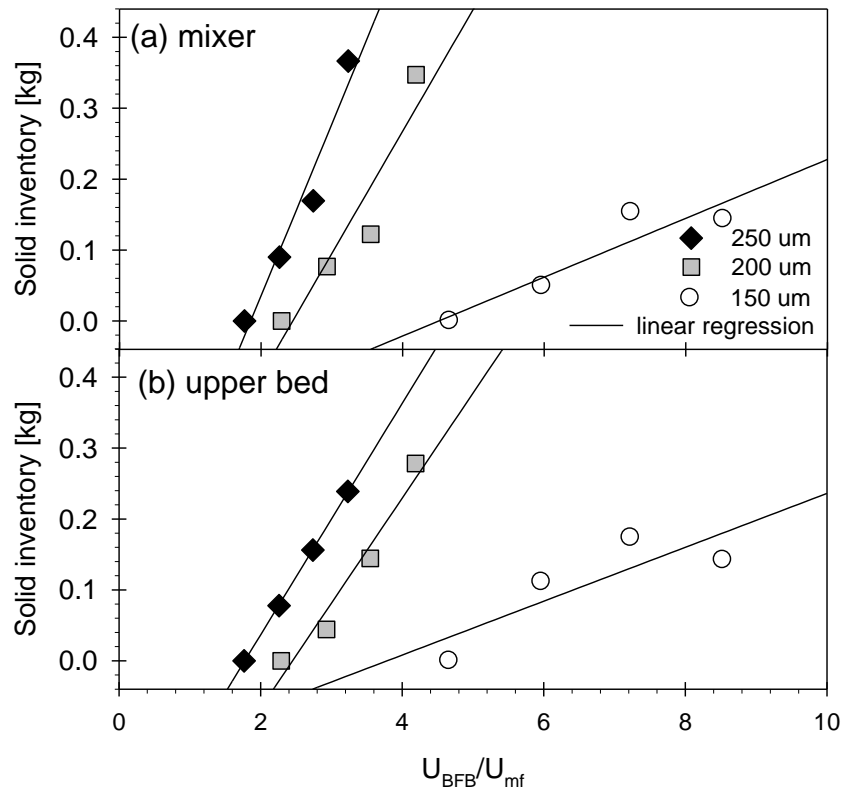


Figure 2.9 Hydrodynamics of bed particles at flow rate of 350 ft³/hr at (a) the mixer and (b) the upper bed

The Figure 2.10 and 2.11 show the results of bed hydrodynamic tests at 400 and 450 SCFH of air in the fast bed respectively. Air and argon at 110~200 SCFH were injected into the BFB. Firstly, when 400 SCFH air is injected to the fast bed, the solid hold up of 150 μ m sand increased from 0 to 0.35kg in the mixer, 0~0.31kg in the upper bed. The solid hold up of 200 μ m sand increased from 0 to 0.16kg in the mixer, 0~0.11kg in the upper bed. And, the solid hold up of 250 μ m increased from 0 to 0.29kg in the mixer, 0 to 0.16kg in the upper bed.

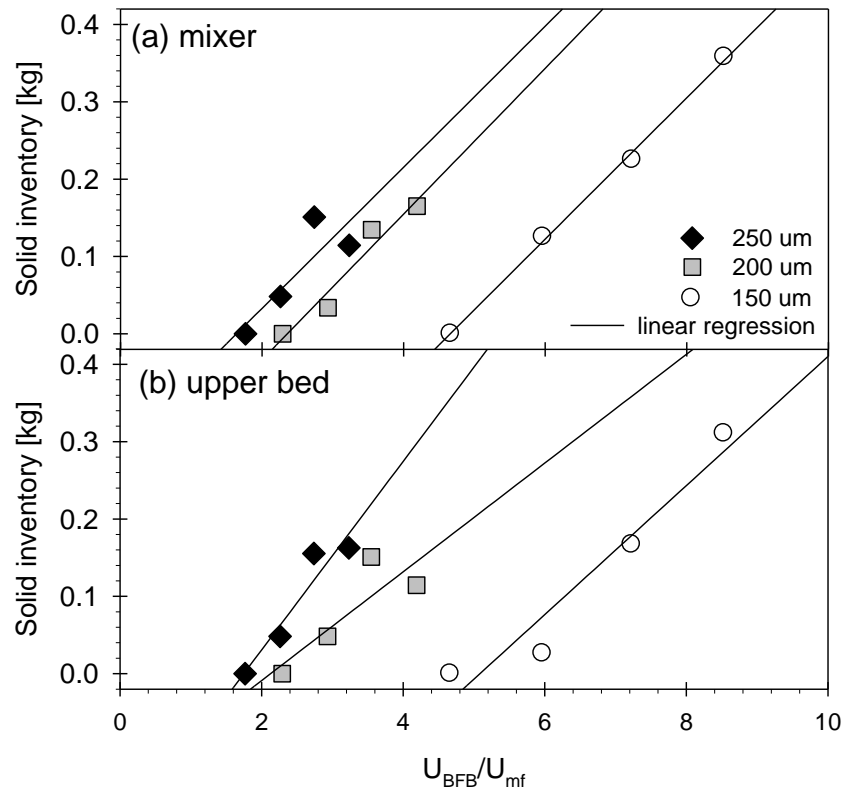


Figure 2.10 Hydrodynamics of bed particles at flow rate of 400 ft³/hr at (a) the mixer and (b) the upper bed

The solid hold up of 150 μ m sand increased from 0 to 0.39kg in the mixer, 0~0.41kg in the upper bed for 450 SCFH air condition as can be seen in Fig. 2.11. The solid holdup of 200 μ m sand increased from 0 to 0.22kg in the mixer 0~0.20kg in the upper bed. And, the solid holdup of 250 μ m sand increased from 0 to 0.24kg in the mixer, 0 to 0.37kg in the upper bed.

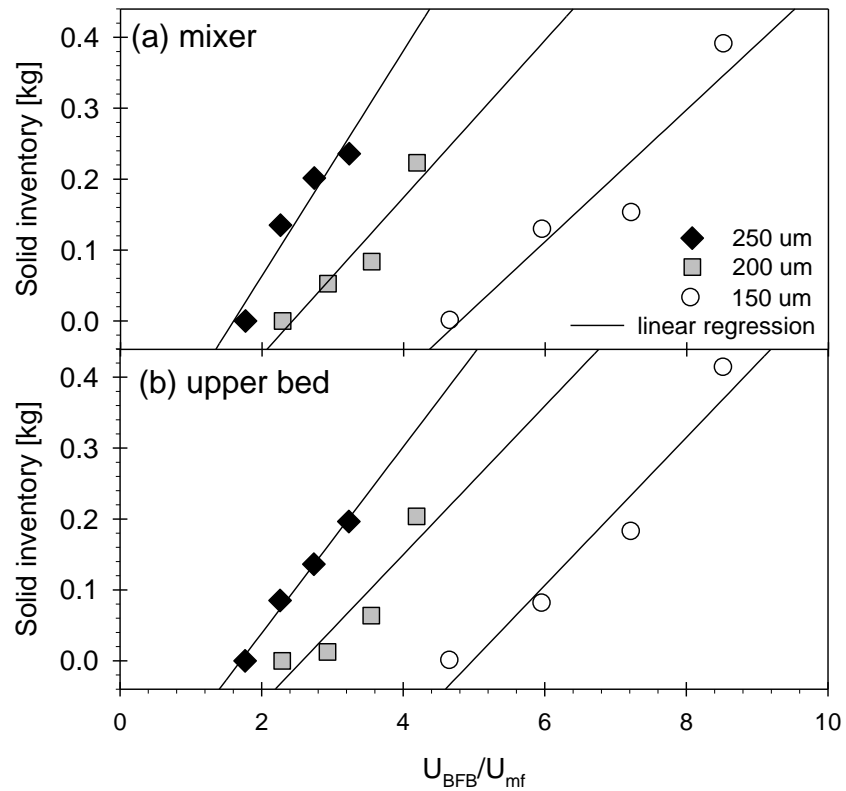


Figure 2.11 Hydrodynamics of bed particles at flow rate of 450 ft³/hr at (a) the mixer and (b) the upper bed

The influence of a change in the superficial velocity in the fast bed was investigated and presented in Fig 2.12. The results show that the higher velocity is in the fast bed (from 350 SCFH to 450 SCFH), more solid is in the fast bed. The increasing solid inventory was found in both the mixer and the upper bed.

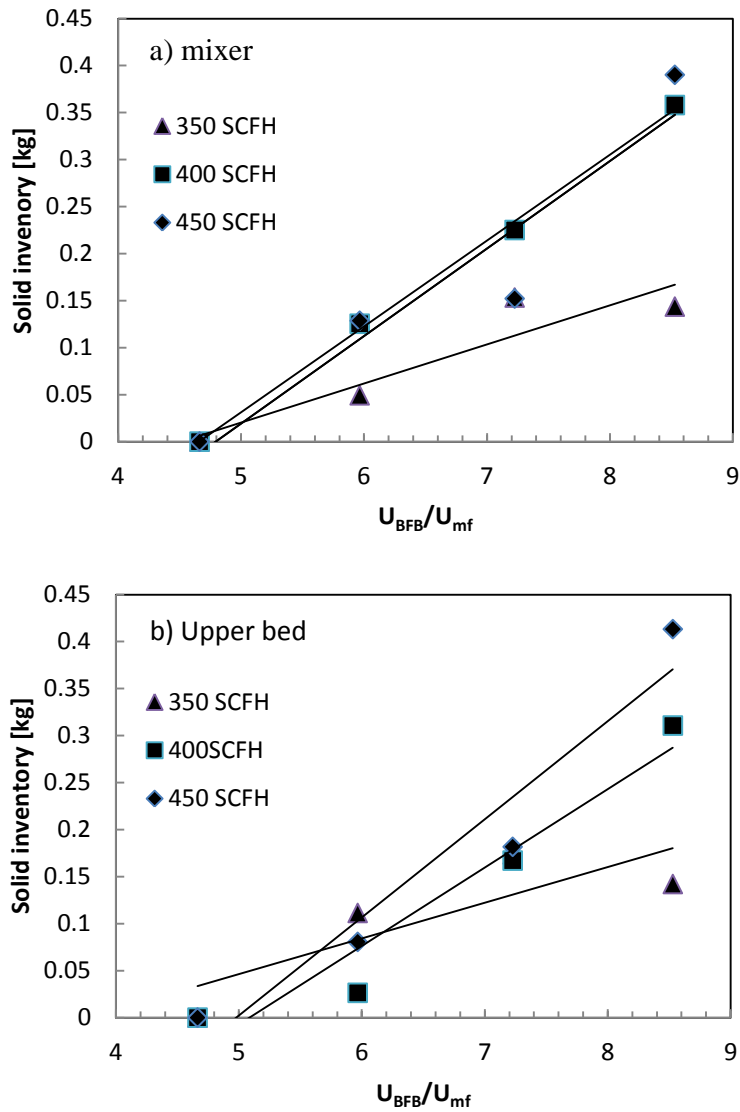


Figure 2.12 Hydrodynamics of bed particles of 150 μ m at flow rate of 350~450 ft³/hr at (a) the mixer and (b) the upper bed

The hydrodynamics study shows that the superficial gas velocity in the BFB and the fast bed and bed particle size influences the flow behavior of bed materials in the DFB.

Increasing gas velocity in both the fast bed and the BFB increased the solid hold up in the

fast bed. Solid hold up in the fast bed (the upper bed and the mixer) increased from 0~0.4kg with increasing gas velocity in the fast bed ($U_{FB}/U_t = 2.3\sim 4.7$) and the BFB ($U_{BFB}/U_{mf} = 1.8\sim 8.5$). And this trend was observed with all of the three groups of sand. The difference in particle size of bed material in the range of 150~250 μm does not have big impact on the hydrodynamics compared to U_{FB} and U_{BFB} .

High volume of solid residing in a gasifier in a DFB during a gasification reaction means high heat and mass transportation for gasification. This is because the solid is the medium for heat transfer. More heat will help ensure to maintain the reaction temperature. And more mass promotes intense solid-gas contacts. Therefore, it is crucial to understand the operation conditions under which heat and mass are supplied to the gasifier. This hydrodynamics study shows that higher superficial velocity in the BFB ($U_{BFB}/U_{mf} = 1.8\sim 8.5$) and fast bed ($U_{FB}/U_t = 2.3\sim 4.7$) lead to more solid inventory in a gasifier. Efficient control of heat and mass in the DFB is available with this information from the hydrodynamics test.

Important observations were gained during the cold model tests along with the results from the mixing and the hydrodynamics test. It was observed that when particles with average size of 250, some of particles in the group settled down at the bottom of the pipe that connects the fast bed and the cyclone. Relatively heavy particles in the two sand groups settled in to form a layer of sand in the pipe. And this resulted in a blockage of the main gas and mass flow. This shows the importance to be aware of the particle distribution of a group of sand. This interruption did not appear in the case of the smallest sand group of 150 μm . This issue is addressed by modifying the pipe installation in the design for DFB. This modification is explained in detail in the next chapter.

2.4 Summary

The design for the DFB allows for an auto thermal system in which the generated heat in a combustor is supplied to gasifier without a need for external heaters. The highly developed design also ensures low degree of mixing of gases between two reactors and low capital and operational costs. SH will show high gasification efficiency in the DFB due to the intense gas- particle contacts. The design advantages and hydrodynamics studies together are to help develop SH process with a high potential for commercialization.

A design of the DFB for SH was proposed and simulated into a cold mode DFB. The mixing test found that the interchange of air and argon was found in the gas stream exiting from the fast bed. The mixing level decreased from 9.4% to 3.8% with an increase in the gas velocity in the fast bed ($U_{FB}/U_t = 3.2\sim 4.7$) and the BFB ($U_{BFB}/U_{mf} = 5.5\sim 6.8$). High solid inventory (11~14kg) also ensured low degree of gas mixing in the DFB. The Gas mixing is minimized at $U_{FB}/U_t = 4.7$, $U_{BFB}/U_{mf} = 6.8$, sand=14kg within the acceptable range. The hydrodynamics test found that increase in the gas velocity in the fast bed ($U_{FB}/U_t = 2.3\sim 4.7$) and the BFB ($U_{BFB}/U_{mf} = 1.8\sim 8.5$) leads to increase in the solid holdup (0~0.4kg) in the fast bed (the upper bed and the mixer). This trend was observed the same with the three sizes of sand.

2.5 Potential implication of this cold model study

The minimum fluidization velocity and the terminal velocity fundamentally characterizes a bed hydrodynamics in a fluidized bed (Miloslav Hartman, 2007).

Hydrodynamics of bed materials are expected to show the same trend under the same flow conditions (U_{FB}/U_t and U_{BFB}/U_{mf}). The flow condition here means the same range of U_t and U_{mf} in the hot mode DFB.

Reference

Daizo Kunii, O.L., Fluidization Engineering. 2nd ed. Chemical Engineering, ed. H. Brenner 1991: Butterworth-Heinemann

T. M. Knowlton, NONMECHANICAL CONTROL OF SOLIDS FLOW IN SINGLE AND MULTI-LOOP SYSTEMS, 2012

Miloslav Hartman,* Otakar Trnka, and Michael Pohor̆ely, Minimum and Terminal Velocities in Fluidization of Particulate Ceramsite at Ambient and Elevated Temperature, Ind. Eng. Chem. Res. 2007, 46, 7260-7266

Sebastian Zimmermann and Fariborz Taghipour*, CFD Modeling of the Hydrodynamics and Reaction Kinetics of FCC Fluidized-Bed Reactors, Ind. Eng. Chem. Res. 2005, 44, 9818-9827

A. Charitos , C. Hawthorne, A.R. Bidwe, L. Korovesis, A. Schuster, G. Scheffknecht, Hydrodynamic analysis of a 10 kWth Calcium Looping Dual Fluidized Bed for post-combustion CO₂ capture, Powder Technology 200 (2010) 117–127

Vaccaro, S., Musmarra, D., Petrecca, M., 1997. Evaluation of the jet penetration depth in gas-fluidized beds by pressure signal analysis. Int. J. Multiphas. Flow. 23 (4), 683–698.

Christoph Pfeifer, Hermann Hofbauer, Development of catalytic tar decomposition downstream from a dual fluidized bed biomass steam gasifier, Powder Technology 180 (2008) 9–16

Takahiro Murakami, Guangwen Xu , Toshiyuki Suda, Yoshiaki Matsuzawa, Hidehisa Tani, Toshiro Fujimori, Some process fundamentals of biomass gasification in dual fluidized bed, Fuel 86 (2007) 244–255

Abbas H. Sulaymon, Ahmed A. Mohammed, Tariq J. Al-Musawi, Predicting the Minimum Fluidization Velocity of Algal Biomass Bed, American Journal of Engineering Research (AJER), Volume-02, Issue-12, pp-39-45

Chapter 3 Modification of DFB design for Stem Hydro-gasification

Design modifications were made for the hot mode DFB based on the hydrodynamics study using the cold mode facility. This modification was made to improve the design to achieve high gasification efficiency and optimize the DFB for SH.

3.1 Design optimization for SH

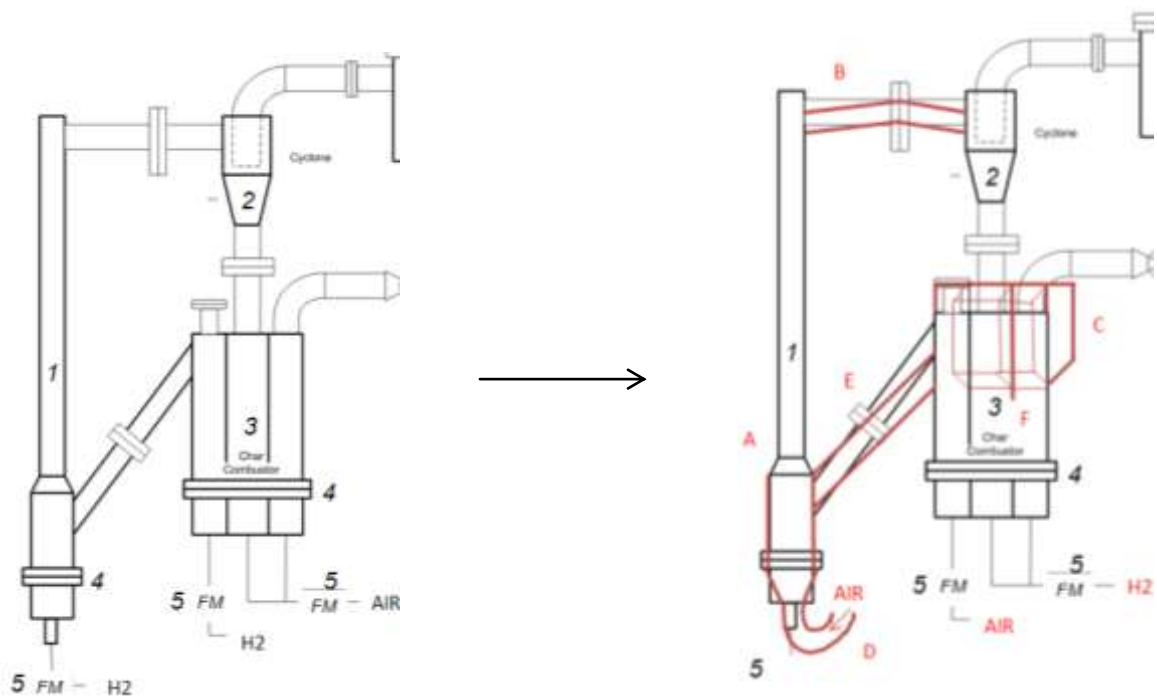


Figure 3.1 Original DFB design and new design with modifications

1. Fast bed (FB) 2.Cyclone 3.Bubbling fluidized bed (BFB) 4. Bag filter 5.Flow Meter (FM) 6.Gas analyser (RGA) 7.Gas distributor

a. A pneumatic riser combustor and a BFB gasifier

There exist many DFB designs that include a BFB for gasification and a fast bed for combustion (Stefan Koppatz, 2009, Guangwen Xu, 2009). The DFB designed and constructed by Ishikawajima-Harima Heavy Industries Co. composes of a BFB gasifier and a pneumatic transported riser (PTR), char combustor (Takahiro Murakami, 2007). Past studies have shown that the DFB consisting of a bubbling fluidized bed gasifier and a pneumatic riser combustor shows superior results regarding gasification reaction and tar formation, when compared to a bubbling fluidized bed combustor and a pneumatic riser gasifier (Guangwen Xu, 2009)

Originally, the fast bed was designed for steam hydro-gasification for its great solid-gas mixing property, and the BFB was designed for combustion within the DFB. However, the BFB is more suitable for SHR than for combustion considering the reaction rate of the two reactions. The feedstock undergoes several steps consecutively in a gasifier; drying, devolatilization, and heterogeneous carbon gasification. Steam hydro-gasification requires minutes-long reaction time in the process. The required reaction time for SH was investigated by previous experimental studies (S.K. Jeon, 2007, Kiseok Kim, 2007, Megha Jayant Patel, 2009). The char and extra fuel are both expected to be completely combusted within a short time in a combustor (Tobias Pröll, 2008). Combustion occurs within a matter of seconds. The bed materials have a longer residence time in the BFB reactor than in the fast bed. The SH reaction occurs for an enough time in the BFB reactor and then the left over char is combusted in the fast bed within seconds. The SH efficiency is expected to improve due to

effective heat transfer with the BFB gasifier and fast bed combustor. The change is presented the Fig 3.1. A.

b. The upper pipe

The upper pipe is the pipe connecting the cyclone and the fast bed. It was observed during the hydrodynamics studies using the cold mode DFB that particles with size over 150 μ m lose its velocity when passing from the fast bed to the upper pipe due to gravity. This resulted in a pile of sand settling in the pipe. This layer of sand eventually caused a blockage of a main flow stream to trigger a flow backward in the system. This caused an over flooding of bed material from the cyclone, losing large quantity of sand particles. This situation not only disturbs the circulation of bed material, but also causes an interchange of two types of gases from two reactors. Mixing of gases from combustion and SHR adversely influences the gasification performance in a hot mode reactor. Carbon conversion efficiency would be very low, and the quality of product gas would be poor due to the introduction of large quantity of CO₂ into the product gas. The suggestion to correct this is to install the upper pipe at a slanted angle. Most of the bed materials are expected to be removed in the pipe installed at a slanted angle. The bed particles would fall into either the fast bed or the cyclone by gravitational force. Here, the degree of angle is not an important factor as long as solid particles fall into either of the two reactors. This design suggestion is depicted in Fig 3.1. B.

c. Bubbling fluidized bed reactor

The volume of the BFB reactor is bigger than the original one in this new design. The change is upper half has a 5 cm bigger diameter than bottom part and the total height of loop seal is extended from 1m to 1.2m. This design modification brings a couple of important advantages. This change is presented in Fig 3.1. C.

A cold model study found that bed particles in the middle and right end compartments in the BFB either escape or flow backwards at a volumetric flow rate of over 200 SCFH. It was found that a group of bed solids flows backward heading to the cyclone in a slugging form instead of falling downward under the condition. This flow backwards toward the cyclone not only impedes the cyclone efficiency but also interrupts the main circulation flow within the DFB. This issue can be addressed with this change in the design. The broader surface area of the upper part prevents bed materials from entraining the reactor in a slugging form. This results in a significantly improved efficiency of the cyclone.

The higher volume of the BFB reactor due to the extension also means more solid inventory in the bed. High solid inventory ensures an efficient heat transfer and an intense solid mixing for SH. This is especially advantageous for SH that has a high water to feedstock ratio of 2. It is because the introduction of the amount of water needs a high and quick heat supply. This is realized by introducing more bed particles that works as a heat carrier.

Lastly, a longer residence time of bed particles in the BFB gasifier is ensured within a larger reactor volume. Steam hydro-gasification can gain benefits from this factor because it requires a minute long reaction time.

d. A distributor

A use of a distributor in a fluidized bed reactor is associated with a maintenance problem. The problem is that carbon or sand particles get stuck in holes of the distributor. This blocks the holes of the distributor and causes the malfunction. This modification can help achieve low maintenance costs. Preliminary tests without a distributor proved that the fast bed functions properly without problem with the change. The change is presented in Fig 3.1 D.

e. A pipe connecting the riser and the BFB

It was found in the cold mode CFB tests that solid flow was often disrupted in the pipe between the two main reactors. It was observed that the solid flow was getting trouble flowing into the fast bed smoothly. This was observed at low solid inventory and high gas velocity in the BFB. Solid and gas flow can be improved by locating the connection pipe 10 cm lower than original place. The solids which were originally falling back to the bottom of the BFB can flow into the lowered pipe to the fast bed. This channels the solids into the pipe without the disruption. The smooth flow of bed materials is beneficial for the DFB operation.

The change will also allow for low solid inventory to function in the system. Previous research found that less than 12 kg of solid inventory in loop seal is not enough to be transported to the riser at around $3 \times U_{mf}$ (m/s) in the case of a bed material with 150 μ m. By lowering the connection pipe, solid particles of low solid inventory will be transported to the riser easily. This suggestion is depicted in Fig. 3.1. E.

f. A partition wall

The cold model study found that the mixing of solids and gases is limited by a partition wall in the BFB reactor. Solid and gas mixing can be improved by removing about 1/5th of the partition wall between the middle and right compartment in the BFB reactor. A larger space is created for the solid-gas mixing in the change. Better mixing between gases and solids will be achieved with less disturbance of the partition wall. The change is illustrated in Fig. 3.1. F.

Reference

Tobias Pröll, Hermann Hofbauer, H₂ rich syngas by selective CO₂ removal from biomass gasification in a dual fluidized bed system — Process modelling approach, FUEL PROCESSING TECHNOLOGY 89 (2008) 1207 – 1217

S.K. Jeon, C.S. Park , C.E. Hackett 1, J.M. Norbeck, Characteristics of steam hydrogasification of wood using a micro-batch reactor, Fuel 86 (2007) 2817–2823

Kiseok Kim, S. K. Jeon, Catherine Vo, Chan S. Park, and Joseph M. Norbeck, Removal of Hydrogen Sulfide from a Steam-Hydrogasifier Product Gas by Zinc Oxide Sorbent, Ind. Eng. Chem. Res. 2007, 46, 5848-5854

Megha Jayant Patel, Design of an Inverted Reactor for Studying the Kinetics of the Steam Hydrogasification Reaction, UNIVERSITY OF CALIFORNIA RIVERSIDE, 2009

Stefan Koppatz , Christoph Pfeifer , Reinhard Rauch , Hermann Hofbauer , Tonja Marquard-Moellenstedt , Michael Specht, H₂ rich product gas by steam gasification of biomass with in situ CO₂ absorption in a dual fluidized bed system of 8 MW fuel input, Fuel Processing Technology 90 (2009) 914–921

Guangwen Xu, Takahiro Murakamia, Toshiyuki Suda, Yoshiaki Matsuzaw, Hidehisa Tani, Two-stage dual fluidized bed gasification: Its conception and application to biomass, FUEL PROCESSING TECHNOLOGY, 90 (2009) 137-144

Guangwen Xu, Takahiro Murakamia, Toshiyuki Suda, Yoshiaki Matsuzaw, Hidehisa Tani, Two-stage dual fluidized bed gasification: Its conception and application to biomass, FUEL PROCESSING TECHNOLOGY, 90 (2009) 137-144

Takahiro Murakami, Guangwen Xu , Toshiyuki Suda, Yoshiaki Matsuzawa, Hidehisa Tani, Toshiro Fujimori, Some process fundamentals of biomass gasification in dual fluidized bed, Fuel 86 (2007) 244–255

Guangwen Xu, Takahiro Murakamia, Toshiyuki Suda, Yoshiaki Matsuzaw, Hidehisa Tani, Two-stage dual fluidized bed gasification: Its conception and application to biomass, FUEL PROCESSING TECHNOLOGY, 90 (2009) 137-144

Chapter 4 Simulation of SH in the DFB and future study

4.1 A heat and mass balance of SH in the DFB

A heat and mass balance of SH in the DFB was calculated using the Aspen plus simulation. Aspen plus is a useful simulation program that can be used to model processes to develop designs and optimize performance (www.aspentech.com). Biomass (pinewood) was chosen as a feedstock for the simulation. The proximate and ultimate analysis of pinewood is presented in Table 4.1.

Table 4.1 Proximate and ultimate analysis of pinewood

	%		%
Moisture	5.65	Carbon	47.56
Volatile matter	81.52	Hydrogen	6.31
Fixed carbon	12.58	Oxygen	45.81
Ash	0.26	Nitrogen	0.05
HHV(BTU/lb)	8093	Sulfur	0.01

Schematic flow diagram of SHR is presented in Fig 4.1. The reaction condition of SH is 800 °C and 400 psi. The reaction condition of combustion is 900 °C and 400 psi. Bed material (sand) transports heat at 900 °C from combustion to SH. The temperature

difference of 100 °C between SH and combustion is to provide the required heat for gasification. Table 4.2 shows the mass balance under the condition.

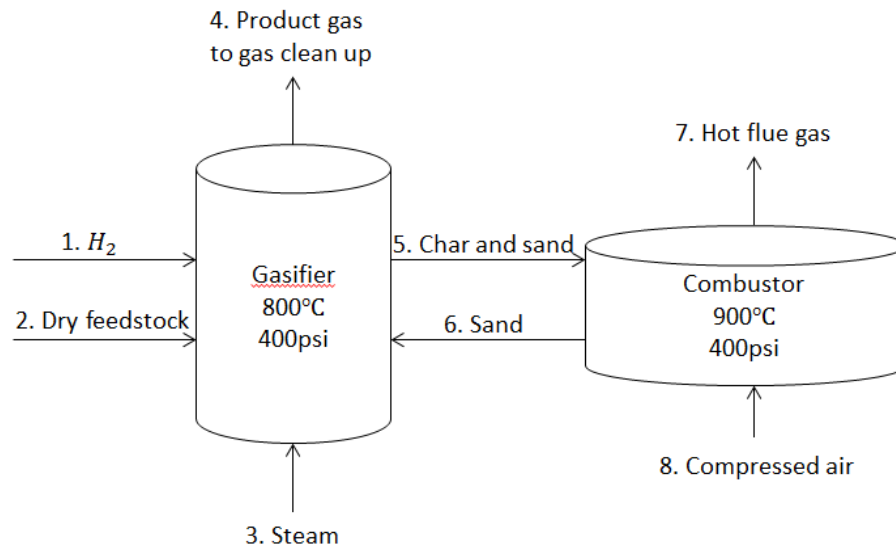


Figure 4.1 Schematic flow diagram of 1TPD SHR with combustor

Table 4.2 Steam tables of simulation results

	Steam number							
	1	2	3	4	5	6	7	8
Temp, °C	324	220	738.6	800	800	900	900	742
Pressure,psi	400	400	400	400	400	400	400	400
Mass flow, kg/day	79	1000	1000	2000	9007	8900	9957	946
H ₂	79			81				
CO				171				
CO ₂				529			240	
CH ₄				256				
H ₂ O (g)			1000	972				
NH ₃				0.608				
H ₂ S				0.106				
O ₂							46	221
N ₂							724	724
Sand					8942	8900		
Char					65			
Pinewood		1000						

The mass balance was obtained with a feed rate of 1 dry ton /day of pinewood.

The combustor burns 13.8% of char which is generated from the gasifier in the presence of 20% excess air. The gasifier net heat duty is -0.4 kw under these conditions.

Table 4.3 Char formation ratio and heat balance at temperature of 700~850 oC (Xiaoming Lu, 2012)

Gasification Temperature(°C)	700	750	800	850
Leftover char (%)	21.7	17.9	13.8	9.2
Gasifier net heat duty (kw)	34	18	-0.4	-20

The heat net duties at different reaction temperatures are summarized in Table 4.3. The char formation ratio in the gasifier was obtained from previous experiments by SH group (Xiaoming Lu, 2012). The temperature ranges from 700~900 °C and pressure is at 400 psi. The higher gasification temperature is the lower net heat duty of the gasifier becomes. This is because less available char for combustion is formed in the gasifier at the higher temperature. Here, the net heat duty is summation of the required amount of energy for SH and the generated amount of energy from combustion. It should be noted that the heat duty in the gasifier is near to zero at 850°C which indicates that the combustion of left over char at this point is sufficient to generate the required heat for SH. That is, the reaction can be run auto thermally under the condition.

4.2. Future study

1) Kinetic studies using a PDU scale fluidized bed

A PDU scale fluidized bed was successfully designed and constructed in our lab at CE-CERT, UCR. Steam hydro-gasification reactions of several feedstocks (biomass, sludge, and food waste) were operated using this reactor. Kinetic studies of SH conducted in this scale of reactor can be compared to the ones conducted in the mini lab scale reactor.

The optimized test conditions verified using the mini fluidized reactor will be used for PDU scale fluidized bed operation. Kinetic behavior of SH in both PDU and mini reactor will be investigated to find out how gasification efficiency is affected by the size of reactor. This task focuses on how the gasification efficiency is influenced when scaling up SHR.

2) Hydrodynamics studies in the cold mode DFB

There are more studies to be carried out to investigate important solid flow behaviors in the configuration in addition to the previously conducted hydrodynamics tests.

- Bed material

Olivine and dolomite are well known catalyst for a gasification reaction for its advantages. These solids are usually used as a bed material as a part of a total solid

inventory. The total solid inventory is made up of catalyst and a majority of sand. The addition of bed particles with different bed density and size to the solid inventory affects solid flow movement in a fluidized bed reactor. It is important to investigate these changes in the behavior and this research will help learn the effects of different bed materials on a gasification reaction.

3) Simulation of SH in the DFB

A mass and energy balance should be carried out using the aspen tool for steam hydro-gasification in both mini fluidized bed and PDU scale fluidized reactor. The simulation results will be compared with the experimental test data. The information obtained from lab and PDU scale fluidized bed tests and the simulation work will be used as the foundational basis of design to develop the PDU scale DFB gasifier.

Reference

Xiaoming lu, Development and Application of Advanced Models for Steam Hydrogasification: Process Design and Economic Evaluation, 2012, University of California, Riverside, 70p

Chapter 5 Summary

Steam hydro-gasification is an endothermic process that needs an external heat supply to operate. Dual fluidized bed reactors may provide efficient heat management. One of the reactors is a gasifier and the other is a combustor. The required heat for steam hydro-gasification can be generated from combustion of the remaining char of the first reactor. The needed heat is transferred to the gasifier through circulation of bed material. In this study a dual fluidized bed reactor is designed for SH. Hydro-dynamics and several studies were carried out using a cold model built. Important results and conclusions from this research are summarized below:

1. Design of a dual fluidized bed reactor and construction of a cold model DFB :

A cold model DFB was built to simulate the gasifier (DFB) for SH. The cold model is made of acrylic plastic. The DFB consists of a fast bed and a BFB. The fast bed is designed as a gasifier and the BFB is designed as a combustor. A gas analyzer is used to analyze the gas streams exiting from the cold model DFB. Fundamental hydrodynamics studies were conducted using this cold model DFB.

2. Mixing and hydrodynamics study using the cold mode DFB :

A mixing test was designed and carried out to observe the mixing level of gases from two reactors (fast bed and the BFB) within the cold DFB. It was observed that the interchange of gases occurred in the

fast bed. No degree of gas mixing was found in the BFB. When the mixing test under different gas conditions was conducted, it was found that the mixing level of gases is influenced by the fluidization parameters. These parameters include the gas velocity in the fast bed and in the BFB and the solid inventory. The mixing level decreased from 9.4% to 4.2 % with an increase in the gas velocity in the fast bed ($U_{FB}/U_t = 3.2\sim 4.7$). The same result was found with an increase in the gas velocity in the BFB. Increasing gas velocity in the BFB ($U_{BFB}/U_{mf} = 5.5\sim 6.8$) resulted in a lower level of gas mixing from 4.8% to 4.2% in the fast bed. The degree of gas mixing also decreased from 5.4% to 3.8% with an increase in the solid inventory from 11~14kg. A high quality of product gas can be ensured by minimizing the gas mixing in this gasifier.

Hydrodynamics studies were designed and conducted following the mixing test. The hydrodynamics experiments were carried out to study the solid movement behavior in the fast bed under differing gas conditions. The main reason to study the solid behavior in the fast bed only is because the fast bed is designed as a gasifier. The solid behavior was observed by measuring the solid holdup in the mixer and the upper bed. The differing gas conditions include gas velocity in the fast bed and the BFB and the average size of solid particles. The results of the hydrodynamics study showed that solid hold up increased 0 to 0.4kg with an increase in gas velocity in the fast bed ($U_{FB}/U_t = 2.3\sim 4.7$) and the BFB ($U_{BFB}/U_{mf} = 1.8\sim 8.5$). The same trend was seen at three different particle sizes of solids (150,200, and 250 μm). The movement of bed materials in the fast bed (gasifier) can be effectively controlled within the DFB with this information. This efficient control of bed solids will ensure high efficiency of steam hydro-gasification.

3. Design improvement : The original design of the DFB was used to build the cold model DFB in order to simulate the gasifier. Several aspects of the DFB which needs improvements were found during the cold mode studies. An improved design was made based on the observations during the studies. The improvement includes a total of 7 changes. The changes are about the fast bed and BFB, 2 pipes within the DFB, the distributor. These changes will improve the DFB gasifier in terms of solid circulation. A high efficiency of steam hydro-gasification is expected in the new DFB with these modifications.

4. Simulation of SH in the DFB : A heat and mass balance of SH in the DFB was calculated using the ASPEN simulation model. Biomass (pinewood) was used as a feedstock. The reaction condition of gasifier is 800 °C and 400 psi. The reaction condition of combustion is 900 °C and 400 psi. Leftover char is 13.8% of total carbon in the feedstock. The leftover char is combusted to generate the necessary heat for SH. The result showed that the required heat for SH is generated from combustion of 13.8% of carbon (1 ton/day pinewood) as char with net heat duty -0.4 kw. The simulation result shows promise for SH process in the scaled up DFB.